

---

This is an electronic reprint of the original article.  
This reprint may differ from the original in pagination and typographic detail.

Tokariev, Maksym; Vuontela, Virve; Lönnberg, Piia; Lano, Aulikki; Perkola, Jaana; Wolford, Elina; Andersson, Sture; Metsäranta, Marjo; Carlson, Synnöve

**Altered working memory-related brain responses and white matter microstructure in extremely preterm-born children at school age**

*Published in:*  
Brain and Cognition

*DOI:*  
[10.1016/j.bandc.2019.103615](https://doi.org/10.1016/j.bandc.2019.103615)

Published: 01/01/2019

*Document Version*  
Peer-reviewed accepted author manuscript, also known as Final accepted manuscript or Post-print

*Published under the following license:*  
CC BY-NC-ND

*Please cite the original version:*  
Tokariev, M., Vuontela, V., Lönnberg, P., Lano, A., Perkola, J., Wolford, E., Andersson, S., Metsäranta, M., & Carlson, S. (2019). Altered working memory-related brain responses and white matter microstructure in extremely preterm-born children at school age. *Brain and Cognition*, 136, 1-14. Article 103615. <https://doi.org/10.1016/j.bandc.2019.103615>

---

This material is protected by copyright and other intellectual property rights, and duplication or sale of all or part of any of the repository collections is not permitted, except that material may be duplicated by you for your research use or educational purposes in electronic or print form. You must obtain permission for any other use. Electronic or print copies may not be offered, whether for sale or otherwise to anyone who is not an authorised user.

# **Altered working memory-related brain responses and white matter microstructure in extremely preterm-born children at school age**

Maksym Tokariev<sup>a,b</sup>, Virve Vuontela<sup>a,b</sup>, Piia Lönnberg<sup>c</sup>, Aulikki Lano<sup>c</sup>, Jaana Perkola<sup>d</sup>, Elina Wolford<sup>e</sup>, Sture Andersson<sup>f</sup>, Marjo Metsäranta<sup>f</sup>, Synnöve Carlson<sup>a,b,g</sup>

<sup>a</sup>Department of Neuroscience and Biomedical Engineering, Aalto University School of Science, Espoo, Finland.

<sup>b</sup>Department of Physiology, Faculty of Medicine, University of Helsinki, Helsinki, Finland.

<sup>c</sup>Department of Child Neurology, Children's Hospital, Pediatric Research Center, University of Helsinki and Helsinki University Hospital, Helsinki, Finland.

<sup>d</sup>Department of Clinical Neurophysiology, University of Helsinki and Helsinki University Hospital, Helsinki, Finland.

<sup>e</sup>Department of Psychology and Logopedics, University of Helsinki, Helsinki, Finland.

<sup>f</sup>Department of Pediatrics, Children's Hospital, Pediatric Research Center, University of Helsinki and Helsinki University Hospital, Helsinki, Finland.

<sup>g</sup>Advanced Magnetic Imaging Centre, Aalto University School of Science, Espoo, Finland.

Maksym Tokariev and Virve Vuontela have equally contributed to this work.

**Corresponding author:** Synnöve Carlson, Department of Neuroscience and Biomedical Engineering, AMI Centre, Aalto University School of Science, P.O Box 13000, FI-00076 AALTO, Finland; e-mail: [synnove.carlson@aalto.fi](mailto:synnove.carlson@aalto.fi)

Short title: Brain imaging of preterm born children

## **Abstract**

Preterm birth poses a risk for neurocognitive and behavioral development. Preterm children, who have not been diagnosed with neurological or cognitive deficits, enter normal schools and are expected to succeed as their term-born peers. Here we tested the hypotheses that despite an uneventful development after preterm birth, these children might exhibit subtle abnormalities in brain function and white-matter microstructure at school-age. We recruited 7.5-year-old children born extremely prematurely ( $< 28$  weeks' gestation), and age- and gender-matched term-born controls ( $\geq 37$  weeks' gestation). We applied fMRI during working-memory (WM) tasks, and investigated white-matter microstructure with diffusion tensor imaging. Compared with controls, preterm-born children performed WM tasks less accurately, had reduced activation in several right prefrontal areas, and weaker deactivation of right temporal lobe areas. The weaker prefrontal activation correlated with poorer WM performance. Preterm-born children had higher fractional anisotropy (FA) and lower diffusivity than controls in several white-matter areas, and in the posterior cerebellum, the higher FA associated with poorer visuospatial test scores. In controls, higher FA and lower diffusivity correlated with faster WM performance. Together these findings demonstrate weaker WM-related brain activations and altered white matter microstructure in children born extremely preterm, who had normal global cognitive ability.

## **Keywords:**

Working memory; pediatric imaging; functional MRI; diffusion tensor imaging; prematurity

## **1. Introduction**

Advances in neonatal healthcare technologies and medical care have increased the survival rate of extremely prematurely born (EPB) children (birth < 28 weeks of gestation) (Seaton, King, Manktelow, Draper, & Field, 2013). These infants are at particular risk of neurodevelopmental and cognitive impairments (Serenius et al., 2013, 2016) that persist through childhood and adolescence (Aarnoudse-Moens, Weisglas-Kuperus, van Goudoever, & Oosterlaan, 2009; Hutchinson, De Luca, Doyle, Roberts, & Anderson, 2013; O'Brien et al., 2004; Johnson et al., 2009; Koivisto et al., 2015) and affect their learning abilities and academic achievement (Taylor, Klein, Minich, & Hack, 2000). Cognitive deficits in children and adolescents born preterm have been associated with impaired executive functions, particularly working memory (WM) (Burnett, Scratch, & Anderson, 2013; Burnett et al., 2018; Mulder, Pitchford, & Marlow, 2010). Preterm birth may have a negative effect on WM abilities (Omizzolo et al., 2013), especially on its visuospatial domain (Clark & Woodward, 2010; Luu, Ment, Allan, Schneider, & Vohr, 2011; Saavalainen et al., 2007). However, cognitive impairments in high-functioning children born extremely prematurely may go unnoticed during the early years of life and become evident only when the children start going to school (Taylor & Clark, 2016). Given that WM is essential for planning, decision-making and learning, and predicts academic attainment in healthy children (Alloway & Alloway, 2010), dysfunction of WM in preterm children may mediate deterioration of academic performance in these children at early school-age (Burnett et al. 2018; Cheong et al., 2017). In the current study, we applied functional magnetic resonance imaging (fMRI) and n-back tasks, and diffusion tensor imaging (DTI) to investigate, in 7.5-year-old children, whether extreme prematurity affected brain activation associated with WM, and the related white matter microstructure.

Working memory is a core cognitive ability that enables holding and manipulating information in mind for short periods of time. The n-back task has been widely used in neuroimaging studies to investigate WM processes. Meta-analyses of n-back task-related brain activations in adults have identified a set of core regions that support WM. These include the dorsolateral, ventrolateral and frontopolar areas of the prefrontal cortex, dorsal cingulate, and lateral and medial premotor and posterior parietal cortices (Owen, McMillan, Laird & Bullmore, 2005; Wang et al., 2019). The areas activated in children and adolescents during n-back tasks are less consistent. A recent meta-analysis of child neuroimaging studies using n-back tasks showed that, like adults, children activate posterior parietal regions quite consistently, as well as the insula and cerebellum, but they show less concordance than adults in frontal activations (Yaple & Arsalidou, 2018). Frontal areas that showed concordant activation during n-back tasks in children included the medial frontal, left superior and inferior frontal gyri, the cingulate cortex and the precentral gyrus. Recently, some studies have suggested that also the hippocampal region is involved in WM, especially during childhood and early adolescence, and that across typical development, the involvement of hippocampal structures in WM decreases (Finn, Sheridan, Kam, Hinshaw, & D'Esposito, 2010; Taylor, Donner, & Pang, 2012; von Allmen, Wurmitzer, & Klaver, 2014).

Few fMRI studies have investigated the neural underpinnings of WM in school-aged children and adolescents born preterm. Impaired WM in 11-year-old children born extremely preterm was associated with reduced activations in fronto-parietal areas (Griffiths et al., 2013, 2014), whereas 13-year-old adolescents born very preterm, compared with controls, had greater activation of the WM network during manipulation of information (Arthursson et al., 2017). In a study on 7-12-year-old children, very preterm-born children activated the right middle frontal gyrus less and the superior frontal gyrus more than controls during WM performance (Mürner-Lavanchy et al., 2014). Moreover, younger and lower performing

preterm children recruited the WM network less than older and better performing preterm children who activated these areas similarly to the controls. These findings, and brain imaging studies on adults born prematurely (Daamen et al., 2015; Kalpakidou et al., 2014; Narberhaus et al., 2009; Nosarti et al., 2009) have led to the suggestion that later brain maturation may involve mechanisms that compensate for the impaired recruitment of WM-related brain areas observed in younger children (Daamen et al., 2015). All in all, knowledge regarding responsiveness of WM-related brain areas, and associations between brain imaging findings and cognitive performance in preterm-born children is still very limited.

An improvement in cognitive abilities during the development is also related to gradual maturation of anatomical connections that transfer the information between brain regions. Diffusion tensor imaging (DTI) of normally developing children has shown that maturation of the white matter is associated with increases in fractional anisotropy (FA) and decreases in mean diffusivity (MD) especially in areas important for attention, memory, cognitive ability and motor skills (Barnea-Golary et al., 2005; Cascio, Gerig, & Piven, 2007). Such changes in the white matter tracts connecting the frontal and parietal regions have been associated with WM development (Darki & Klingberg, 2015; Nagy, Westerberg, & Klingberg, 2004; Vestergaard et al., 2011; Østby, Tamnes, Fjell, & Walhovd, 2011). Preterm birth, however, may affect the maturation of the white matter (Volpe, 2009). In children, adolescents and adults born preterm, compared with controls, reduced FA values have been reported in several tracts important for cognitive and motor functions such as the superior and inferior longitudinal fasciculus (SLF, IFL), inferior fronto-occipital fasciculus (IFO), corpus callosum (CC), and cortico-spinal tract (CST) (Eikenes, Løhaugen, Brubakk, Skranes, & Håberg, 2011; Li et al., 2015; Skranes et al., 2007; Vangberg et al., 2006; Vollmer et al., 2017). Some studies, however, found no significant differences in the measures of white matter microstructure (Duerden, Card, Lax, Donner, & Taylor, 2013; Loe, Lee, & Feldman, 2013),

or reported higher FA values (Feldman et al. 2012), or both higher and lower FA values in preterm compared with term-born subjects (Allin et al., 2011; Li et al., 2015). Lower FA values in preterm children and adolescents have been associated with impaired attention (Loe et al., 2013; Murray et al., 2016) and executive functions including WM (Skranes et al., 2009; Vollmer et al., 2017), and lower IQ (Skranes et al., 2007), whereas no associations between FA values and IQ were found in a recent study on very preterm children (Young et al., 2018).

Maturation of the gray and white matter of the fronto-parietal network has been related to improvements in WM in typically developing individuals using both fMRI and DTI (Darki & Klingberg 2015; Olesen, Nagy, Westerberg, & Klingberg, 2003). Few studies on preterm-born populations applied both fMRI and DTI. In these studies, preterm newborns showed distinctive cortical responses to linguistic stimuli and delayed white matter development of language-related neural tracts (Baldoli et al., 2015), and adults born very preterm had an altered pattern of activations in a network of brain regions supporting the performance of verbal learning tasks, and abnormalities in the related neural tracts (Salvan et al., 2014). DTI has also been used in combination with resting-state fMRI to investigate the structural and functional connectivity of brain networks (Cui et al., 2017; van den Heuvel et al., 2015; Weinstein et al., 2016) that in school-aged preterm children showed less connectivity and complexity than in their term-born peers (Thompson et al., 2016). To our knowledge, no earlier studies on preterm born children investigated WM-related brain activation and the microstructure of the underlying white matter tracts.

In the present study, we focused on a relatively homogenous group of high-functioning, extremely preterm-born children with a narrow age range. With “high-functioning” we refer to children whose cognitive performance, based on a neuropsychological assessment at 6 years, was within normal range, and who have no neurological or neurosensory impairments. We investigated whether these children, at school-age, have subtle abnormalities in brain

function and white-matter microstructure. We recruited 7.5-year-old EPB children, who had mild or no signs of brain injury in MRI at term equivalent age (Table 1), and age- and gender-matched controls born at term. We applied the blood-oxygen-level-dependent (BOLD) fMRI to investigate activation patterns while the children performed visuospatial n-back tasks that require selective attention, maintenance and manipulation of information. We also used DTI to evaluate the microstructure of the white matter. We were interested in the following research questions: 1) Do well striving EPB children show different neuronal activations during the n-back tasks compared with age-matched TB children; 2) do DTI measures differ between the two groups; and 3) do the brain imaging measures correlate with task performance and neuropsychological test scores. Based on the current literature, we hypothesized that if group differences in the brain measures were observed, they would be the following: i) The EPB children might show decreased or increased (compensated) activations during n-back tasks especially in the prefrontal cortical areas that are important in WM. ii) EPB children, compared with TB children, might exhibit lower FA and higher diffusivity, especially in neural tracts important for cognitive and motor functions. Finally, iii) we also hypothesized that the BOLD signal in the prefrontal cortex would correlate with the level of task performance, and higher FA and lower diffusivity with better performance in n-back tasks and neuropsychological tests.

## **2. Materials and Methods**

### *2.1. Participants*

The participants were from a cohort of children originally recruited for a larger multi-methodological follow-up study (KeKeKe, Extremely Preterm Birth and Development of the Central Nervous System, Rahkonen et al., 2013, 2014) and prospectively followed since birth.

The EPB children (< 28 weeks of gestation) were born between 2006 and 2008, and treated after birth at the neonatal intensive care unit of the Helsinki University Central Hospital, Finland. The term-born (TB) children ( $\geq 37$  weeks of gestation), including 8 new controls recruited at 6 years of age, were born healthy between 2006 and 2009 in the Hospital District of Helsinki and Uusimaa, Finland. Exclusion criteria for EPB children were grade III-IV intraventricular hemorrhage, white matter injury, chromosomal abnormality, global cognitive impairment, cerebral palsy, attention deficit hyperactivity disorder (ADHD), insufficient native language skills, mutism and metal in body. These exclusion criteria were defined to recruit a study group of children as homogeneous as possible and to enable participation to both fMRI and neuropsychological examinations. The TB children had no known brain abnormalities, neurological or neuropsychiatric disorders. Inclusion and exclusion criteria and drop-outs for all children are summarized in Fig. 1. All children were European, of Finnish nationality, and attended normal elementary schools. The participants underwent an ophthalmological examination and all had normal or corrected to normal vision with no strabismus.

Altogether 21 EPB children who met the inclusion criteria and 21 TB children were enrolled for structural and functional MRI. Subsequently, several children were excluded from the analyses resulting in 16 EPB and 16 TB children, whose data were analyzed (Fig. 1). Finally, the fMRI data of the n-back tasks were analyzed for 14 EPB (8 males) and 14 TB (7 males) children and DTI data for 15 EPB (8 males) and 16 TB (9 males) children. Details of the clinical characteristics of the children in the two study groups are summarized in Table 1, and a detailed description of the evaluation of EPB children's MRIs at term equivalent age in Supplementary Table 1.

Ethical approval for the study was obtained from the Ethics Committee for Gynecology and Obstetrics, Pediatrics and Psychiatry of the Hospital District of Helsinki and Uusimaa.

All children gave assent and caregivers provided informed written consent prior to participation in accordance with the Declaration of Helsinki.

## *2.2. Clinical data*

Perinatal data were collected from hospital records and parental questionnaires. General cognitive ability (full-scale intelligence quotient, FSIQ) was assessed using three Performance (Block Design, Matrix Reasoning, and Picture Completion) and two Verbal (Information and Vocabulary) subtests of the Finnish edition of the Wechsler Preschool and Primary Scale of Intelligence, Third Edition, WPPSI-III (Wechsler, Heiskari, Jakobson, & Marila, 2009). The TB children, compared with the EPB group, had higher scores in age-scaled (mean 100, SD 15) Performance IQ ( $P = 0.02$ ), and there was a trend for higher scores in age-scaled FSIQ ( $P = 0.07$ ) (Table 1). Visual attention (Visual attention test), visual memory (Memory for designs) and visuospatial processing (Arrows and Block construction) were measured using age-scaled scores (mean 10, SD 3) from tests of the Finnish edition of the neuropsychological assessment tool NEPSY, Second Edition (NEPSY-II) (Korkman, Kirk, & Kemp, 2008). EPB children did not differ significantly from the TB children in their visual attention and memory skills but had lower visuospatial scores than TB children. However, all age-scaled scores measuring cognitive ability and visuospatial processing of the EPB children were within normal range (Table 1). Handedness was determined based on neurological examination and neuropsychological tests. Maternal education was obtained by a parental questionnaire.

## *2.3. Visuospatial n-back tasks during fMRI*

Children performed visuospatial n-back tasks with three load levels (0-, 1-, and 2-back tasks). The 0-back task requires sustained attention but no WM, whereas 1-back and 2-back tasks measure WM (Owen et al., 2005). The stimuli (duration 200 ms, interstimulus interval 1700 ms) were small white squares (100 x 100 pixels, subtending a visual angle of 4°) presented

randomly in eight possible locations at an eccentricity of about 8.2° around a central visual fixation cross (Fig. 2A). The child was instructed to press the left button of a response pad with his/her right index finger whenever the stimulus in the 0-back task occurred in a predetermined location (left upper corner), in the 1-back task in the same location as the previous one, and in the 2-back task in the same location as two trials back, and the right button with the right middle finger if it was in a different location. The children were instructed to respond as fast and as accurately as they could. In addition to the tasks, there was a rest condition (R) during which no stimuli were presented and no task was performed. In all tasks and in the R condition, the children were instructed to fixate a central visual fixation cross.

The tasks were presented in a block design. The children performed three separate runs in total, each containing two blocks of 0-, 1- and 2-back tasks and R conditions in a semi counterbalanced order. Each block started with the presentation of a central visual fixation cross for 2200 ms. Then, an instruction figure (2200 ms) indicated the nature of the ensuing block (0-, 1-, or 2-back task or R-condition). After a 5600-ms interval of visual fixation, a block of 16 trials of the task condition followed. Thus, 96 trials of each task condition were performed during the experiment resulting in a total of 288 trials. The duration of one run was 5 min 58 s. A short break was held between the runs during which the child stayed in the scanner and was reminded to stay still. A computer program (Presentation, Neurobehavioral Systems, Inc.) presented the stimuli and collected the behavioral data (response times (RTs), correct, incorrect, missed, and multiple responses).

Before entering the scanner, the n-back tasks were explained and the child was allowed to practise until he/she understood the nature of the tasks. This was controlled by checking the log file of the performance. On average, children practised 23 trials of each task. After the imaging session, the children completed a questionnaire designed to evaluate their level of

alertness during the scanning, and the task difficulty. A two-way repeated-measures ANOVA showed that there were no significant differences in the reported alertness during scanning between the groups (see Supplementary results 1).

#### *2.4. Behavioral data analysis*

Task performance level in both groups was assessed by using the percent incorrect responses and RTs. These behavioral measures and the difficulty evaluation were analyzed using a two-way ANOVA with repeated measures with group as the between subjects factor and task (0-, 1- and 2-back) as the within subjects factor (StatSoft Statistica, [www.statsoft.com](http://www.statsoft.com)). The significance level was set at  $P < 0.05$ . If the ANOVA gave a significant main effect ( $P < 0.05$ ), planned contrasts (with Bonferroni correction) were performed.

#### *2.5. MRI data acquisition*

Scanning was performed at the Advanced Magnetic Imaging Centre of Aalto University using a 3 T MAGNETOM Skyra scanner (Siemens Healthcare, Erlangen, Germany) and a 30-channel head coil. To avoid fatigue, the imaging was conducted in two successive sessions with a break between them during which the child was let out from the scanner, offered refreshments and rest. First, a high-resolution T1-weighted MRI scan was acquired using a MPRAGE sequence (176 sagittal slices, FOV 256 mm, matrix size 256 x 256, 1.0 mm isotropic voxels). Then, functional images were obtained during n-back task performance using a gradient-echo echo-planar imaging (EPI) sequence (TR 2500 ms, TE 30 ms, flip angle 75°, FOV 220 mm, matrix size 64 x 64, in plane resolution 3.5 x 3.5 mm). Each functional volume consisted of 45 axial slices of 3.5 mm thickness with no inter-slice gap covering the whole cerebrum and cerebellum. The first imaging session lasted about 40 min and included a 6-min resting state dataset collected at the end of the session, the results of which will be reported elsewhere. In the second imaging session, diffusion-weighted images were acquired

using a spin-echo-based single shot EPI sequence with full k-space coverage and GRAPPA parallel acquisition option (TR 9000 ms, TE 80 ms, FOV 240 mm, matrix size  $96 \times 96$ , slice thickness 2.5 mm, 70 contiguous axial slices). The DTI dataset (45 volumes: 30 uniformly distributed diffusion gradient directions at  $b=1000 \text{ s/mm}^2$ , 6 directions at  $b=500 \text{ s/mm}^2$ , 6 directions at  $b=300 \text{ s/mm}^2$ , and 3 non-diffusion-weighted images at  $b=0 \text{ s/mm}^2$ ) was collected twice with reversed phase-encoding directions (anterior-posterior and posterior-anterior). For each subject, T2-weighted images were obtained using SPACE sequence (TR 3200 ms, TE 411 ms, FOV 256 mm, matrix size  $256 \times 256$ , 176 sagittal slices, 1.0 mm isotropic voxels). The children were shown video movies during the second imaging session that lasted approximately 25 min.

## *2.6. MRI data analysis*

Functional MRI data were analyzed with FSL 5.0 (FMRIB's Software Library, Oxford, UK). Prior to any preprocessing, the FSL Motion Outliers script was run on the 4D dataset to create a confound matrix of time points corrupted by intermediate/large motion to be used in the GLM to remove their effect on the analysis. Preprocessing included brain extraction, motion correction (rigid-body transformations), high pass filtering (cut off period 170 s) and spatial smoothing (5 mm FWHM Gaussian kernel). Motion parameters (three rigid-body translations and three rotations) for the three runs of fMRI data were examined in each child individually to ensure that the absolute motion did not exceed the dimensions of a normalized voxel (2 mm). A two-way repeated-measures ANOVA showed no significant differences in the absolute motion between the groups (main effect of group:  $F(1,26) = 0.06$ ,  $P = 0.807$ ). Registration to the individual's structural MRI and to the standard image was carried out using FLIRT (Jenkinson, Bannister, Brady, & Smith, 2002; Jenkinson & Smith, 2001).

Statistical maps of each child's functional time series data were generated via multiple regression analyses computed for each voxel.  $Z$  (Gaussianized  $F$ ) statistic images were thresholded using clusters determined by  $Z > 2.58$  corresponding to  $P < 0.005$ , to balance between Type I and II error rates (Lieberman & Cunningham, 2009), and a Gaussian Random Field (GRF)-theory-based corrected cluster significance of  $P < 0.05$  (Worsley, Evans, Marrett, & Neelin, 1992). We used three regressors to model each of the three task conditions (0-, 1- and 2-back) and a confound matrix to model the effect of timepoints corrupted with motion on the analysis. The R condition was the unmodeled baseline. Task-related regressors were convolved with the double Gamma HRF model.

Contrast images comparing n-back tasks with the visual fixation baseline were computed for each task condition in each child and separately for the TB and EPB groups. Contrasts 1-back > R and 2-back > R were used to detect the WM network as the performance of 1- and 2-back tasks requires on-line monitoring, updating and manipulation of retained information. Contrast 0-back > R probes brain activation related to attention as the 0-back task requires the detection of a predetermined stimulus but does not demand manipulation or memorizing of the stimuli presented earlier (Owen et al., 2005). The effect of WM load increase on brain activation was investigated by contrasting the two WM tasks (2-back vs. 1-back).

To find significantly activated brain areas at the group level, we used FLAME (Beckmann, Jenkinson, & Smith, 2003) of the FSL toolbox with mixed effects modeling and the thresholding of  $Z > 2.58$  and GRF corrected cluster  $P < 0.05$ . WM load effects (2-back vs. 1-back) and group differences were examined using a repeated measures two-way ANOVA with mixed effects modeling. With this model, we tested for the main effect of load and the interaction of group x load. The group effect was modeled by means of a two sample unpaired t-test ([fsl.fmrib.ox.ac.uk/fsl/fslwiki/GLM](http://fsl.fmrib.ox.ac.uk/fsl/fslwiki/GLM)).

### *2.7. fMRI ROI analysis*

In order to investigate the BOLD signal in the two groups in task-relevant brain regions, we performed a ROI analysis. We focused on frontal regions that have shown concordant activation during n-back tasks in children in medial and lateral PFC, and in the insula (Yaple & Arsalidou, 2018). To avoid selection bias on the results (Kriegeskorte, Simmons, Bellgowan, & Baker, 2009), the ROIs were defined based on a combined activation map that consisted of all task contrasts (0-back > R, 1-back > R, 2-back > R) of the voxelwise whole-brain analysis including all children from both groups. This analysis identified WM-related regions that were consistent with the frontal regions described in the meta-analysis of Yaple & Arsalidou (2018). We drew a spherical ROI with an 8-mm radius to cover the bilateral medial PFC (PFCmed) that also included voxels in the anterior cingulate cortex. Two other spherical ROIs (6-mm radius) were drawn to regions in the left dorsolateral PFC (PFCdl) and to the right insular/opercular cortex (InsOper). All three ROIs included the local maximum of the voxel cluster. From each ROI, we extracted the mean percent signal change in the three task conditions for each child. The signal changes in the 0-, 1- and 2-back tasks in these ROIs in EPB and TB children are presented in the Supplementary material (Supplementary Figure 1).

To test whether BOLD responsivity of these ROIs was associated with WM performance, we correlated the mean BOLD signal values of each ROI in each child with incorrect responses in the 1-back and 2-back WM tasks.

### *2.8. DTI data preprocessing and analysis*

DTI data preprocessing was carried out with TORTOISE 2.5.2b software (<http://www.tortoisediti.org>) (Pierpaoli et al., 2010). The DTI datasets in both phase encoding directions were corrected for motion artefacts, eddy currents and EPI distortions, and the b-

matrix was reoriented to preserve the orientation information (Supplementary Methods 1). The output images with reversed phase encoding directions were combined within the TORTOISE DR-BUDDI (Irfanoglu et al., 2015) module which corrects for susceptibility induced EPI distortions, and the corrected DTI dataset was produced for each child for further analysis. The tensors were estimated with the nonlinear RESTORE algorithm (Chang, Jones, & Pierpaoli, 2005) and then spatially normalized to the population-specific DTI template using the DTI-TK (<http://dti-tk.sourceforge.net>) (Zhang et al., 2007) registration toolbox (Supplementary Methods 1). The results of the DTI-TK registration pipeline are illustrated in Supplementary Figure 2. Following normalization, Tract-based Spatial Statistics (TBSS) (Smith et al., 2006) analysis was carried out in FSL 5.0. The mean FA volume was generated and thinned to produce the white matter skeleton (thresholded at a mean FA value of 0.2). The children's spatially normalized FA maps were forwarded to the final steps of the TBSS pipeline. Individual datasets were projected onto the skeleton and the voxelwise statistical analysis of the FA values was carried out. Additionally, the DTI-TK toolbox was used to generate the maps of MD, axial diffusivity (AD) and radial diffusivity (RD) for each child. The group differences in the white matter measures were estimated using an unpaired *t*-test with nonparametric permutation method with 5000 permutations. Statistical maps were thresholded at  $P < 0.05$  using a threshold-free cluster enhancement (TFCE) method with family-wise error (FWE) correction for multiple comparisons.

Whole brain analyses of possible correlations between FA, MD, AD and RD values and the measures of WM task performance (RTs, incorrect response rate) were conducted for each group. The correlation analyses for each group were also performed between the aforementioned measures of the white matter microstructure and the age-scaled neuropsychological test scores of visual memory, visual attention, and visuospatial

processing. The maps of positively and negatively correlated voxels were thresholded at  $P < 0.05$  using the TFCE method with correction for multiple comparisons.

### 3. Results

#### 3.1. Performance of the 0-, 1-, and 2-back tasks

Figure 2B shows the average RTs and incorrect responses of the EPB and TB children in the 0-, 1-, and 2-back tasks. A two-way repeated measures ANOVA of the RT data showed significant main effects of Group ( $F(1,26) = 4.55, P = 0.043, \text{partial } \eta^2 = 0.15$ ) and Load ( $F(2,52) = 23.58, P < 0.0001, \text{partial } \eta^2 = 0.48$ ), but no interaction between Load and Group (Fig. 2B). The TB children performed all tasks slower than EPB children, and both groups performed the 0-back tasks faster than the 1-back ( $t(26) = 5.93, P = 0.0003, \text{Cohen's } d = 2.33$ ) and 2-back ( $t(26) = 5.69, P = 0.0003, \text{Cohen's } d = 2.23$ ) tasks. The EPB children made significantly more mistakes than TB children (main effect of Group,  $F(1,26) = 8.77, P = 0.006, \text{partial } \eta^2 = 0.25$ ). Both groups made more incorrect responses in the higher than lower task loads (main effect of Load:  $F(2,52) = 27.22, P < 0.0001, \text{partial } \eta^2 = 0.51$ ) but the Load x Group interaction was not significant (Fig. 2B). In the 2-back task, the RTs of the TB children correlated negatively with the number of incorrect responses (Spearman's  $r_s = -.733, P = 0.009$ ) indicating that slower responses were associated with better performance. We also tested the association between RT and incorrect responses over all children (TB + EPB) and found a negative correlation between RTs and the number of incorrect responses in both 1-back (Spearman's  $r_s = -.556, P = 0.006$ ) and 2-back (Spearman's  $r_s = -.614, P = 0.003$ ) tasks.

Subjective evaluation of task difficulty level showed that both groups of children evaluated 2-back tasks as the most difficult and 0-back tasks as the easiest ones (main effect of Load:  $F(2,52) = 37.66, P < 0.0001, \text{partial } \eta^2 = 0.59$ ).

### *3.2. fMRI activation during tasks*

#### *3.2.1. Within-group activations*

The within-group whole brain analysis, contrasting the 0-, 1- and 2-back tasks with fixation baseline, showed that TB children activated a network of frontal and parietal brain areas whereas EPB children activated a similar network but the clusters were fewer (Fig. 3A,B, Supplementary Table 2). In TB children, the BOLD activation increased from 0-back to 1-back to 2-back task whereas in EPB children activation increased from 0-back to 1-back task but not from 1-back to 2-back task (Fig. 3A,B). During WM tasks (1-back and 2-back), TB children activated bilaterally several areas of the prefrontal (middle frontal (MFG), superior frontal (SFG), precentral (PreCG), frontopolar (FP) and cingulate (CingG) gyri, and insula (Ins)), and parietal (superior parietal lobe (SPL), supramarginal gyrus (SMG)) cortices (Supplementary Table 2). Like TB children, EPB children activated several prefrontal and parietal areas bilaterally in the 1-back task (MFG, SFG, PreCG, Ins, SPL and SMG) but in the 2-back task, the activation was mainly in the left hemisphere (Supplementary Table 2). In TB children, direct contrasts between the 2- and 1-back tasks showed WM load-related increase of brain activity in the right SFG and MFG, and in precuneus (PreCun), SPL and posterior CingG (CingGpost). No areas in EPB children increased activation from 1-back to 2-back task (2-back > 1-back) (Fig. 3B; Supplementary Table 2).

#### *3.2.2. Between-group differences*

Analysis of group differences in the 0-back task-related activations showed stronger responses in TB than EPB children in the right FP, including an area in the orbitofrontal cortex (OFC), and in the cerebellum (Cer) extending to parahippocampal gyrus (PHG). No areas were more activated in EPB than TB children during the 0-back task (Fig. 3C; Supplementary Table 3).

WM load-related activation patterns and group differences were further examined with an ANOVA of the whole-brain data. The results showed a significant main effect of Load ( $F(1,26) = 1.03, P < 0.005$ ) in PreCun that was activated more during 2-back than 1-back task (Supplementary Table 3). During WM tasks (1-back + 2-back), several prefrontal regions, including areas in the right OFC, MFG, FP and Ins, were activated more in TB than EPB children. EPB children, on the other hand, exhibited stronger activation than TB children in the right temporal lobe, including areas in the temporal pole (TP), PHG, hippocampus (Hipp), superior temporal (STG) and fusiform (FG) gyri, (two sample unpaired  $t$ -tests,  $P < 0.005$ ). There was no interaction between Load and Group.

To understand the basis of the stronger activation of the right temporal lobe regions in EPB than TB children, we drew a ROI that covered all differentially activated voxels (EPB > TB) and investigated the mean signal change within this ROI in the WM tasks (Supplementary Methods 2). The results showed that both groups of children deactivated this area during 1-back and 2-back tasks but the deactivation was stronger in TB than EPB children (Fig. 3E).

### *3.3. Associations between brain activation and behavior*

To investigate whether WM performance accuracy had an association with the brain activation level, we correlated the mean BOLD signal values of the task-related frontal areas that in children showed concordant activation in the meta-analysis during n-back tasks (Yaple & Arsalidou, 2018) with the incorrect responses in the 1-back and 2-back WM tasks. In EPB children, better accuracy in the 2-back task was associated with higher mean BOLD signal in the PFCmed (Spearman's  $r_s = -.732, P = 0.004$ , after Bonferroni correction with 6,  $P = 0.024$ ) and left PFCdl ( $r_s = -.641, P = 0.018$ , not significant after Bonferroni correction) (Fig. 4).

### *3.4. Group differences in FA, MD, AD, and RD*

The TBSS analyses suggested larger FA values in the EPB group compared with the TB group within a set of white matter regions including the SLF, ILF, IFO, CST, and CC (TBSS,  $P < 0.05$ , TFCE corrected, Fig 5A). There were no regions of higher FA values in TB compared with EPB children. As this result differs from several earlier studies on prematurely born individuals, we checked the validity of the TBSS result and performed three additional tests; a split sample analysis (Bach et al., 2014) that looked for unexpected false positives, a TBSS analysis using FSL registration, and an analysis that looked for potential outliers (Supplementary Methods 3, Supplementary Figure 3). These additional analyses detected no false positives or potential outliers, and the group comparisons indicated that the EPB children had higher FA values than the TB children. The TB compared with EPB group demonstrated higher MD and RD values in several of the white matter regions (bilateral SLF, IFO/ILF, CST and inferior cerebellar peduncle) that showed larger FA values in EPB (Fig. 5B,D). The TB group also demonstrated higher AD values than the EPB group in bilateral anterior thalamic radiation, CST and left ILF and SLF (Fig. 5C).

### *3.5. Associations of white matter microstructure with WM performance and neuropsychological tests*

In TB children, the whole brain analysis showed a negative correlation between FA values and the 1-back and 2-back RTs ( $P < 0.05$ , TFCE corrected). Higher FA values were associated with faster RTs within the right SLF, bilateral CST, and in 1-back task, within bilateral IFO/ILF (Fig. 6A,B). The TB children also showed significant positive associations between MD and RD values and the 1-back RTs ( $P < 0.05$ , TFCE corrected) such that in several white matter tracts, faster RTs were related to lower MD and RD values (Fig. 6A).

There were no associations between FA, MD, AD or RD values and WM performance in EPB children.

The analyses of associations between the whole-brain white matter microstructure and neuropsychological test scores showed a significant positive correlation in the TB children between MD, AD and RD values and the number of errors in the visual attention test (total inattention errors) such that higher diffusivity values were related to higher number of errors in white matter regions including the bilateral SLF, IFO/ILF and CST (Fig. 7A). The EPB children showed a significant negative correlation between the FA and the age-scaled scores of the visuospatial processing test (Block construction) in the right cerebellar white matter (Fig. 7B). There were no correlations between visual memory scores and DTI measures in either of the groups.

#### **4. Discussion**

The current study applied functional MRI and DTI on high-functioning 7.5-year-old children born extremely prematurely, and on age-matched controls. EPB children, compared with TB children, had reduced cortical responsiveness in frontal WM-related brain areas, weaker deactivation of task-unrelated right temporal lobe structures, and increased FA and decreased diffusivities in several neural tracts important for cognitive and motor functions. Furthermore, the weaker the activation in the prefrontal cortex of the EPB children, the poorer they performed the WM tasks.

##### *4.1. N-back task performance and brain responsiveness*

The EPB children made more mistakes and, interestingly, performed the n-back tasks faster than TB children. Earlier studies in normally developing 6–13-year-old children have demonstrated that visuospatial n-back task performance improves with age; RTs get shorter and accuracy increases (Aronen, Vuontela, Steenari, Salmi, & Carlson, 2005; Vuontela et al.,

2003). However, the youngest children (6–8-year-olds) performed 2-back tasks faster and less accurately than the older children which was suggested to be due to the younger children being more impulsive and less capable of inhibitory control (Vuontela et al., 2003). In the current study, TB children had a negative correlation between RTs and incorrect responses in the 2-back task, and when this correlation was examined over all children, faster performance associated with lower accuracy in 1-back and 2-back tasks (see Results 3.1). The finding that EPB children performed the tasks faster and made more mistakes than TB children suggests that their cognitive control systems that develop gradually over childhood (Dempster, 1992), were less mature than in their age-matched controls.

In the n-back tasks, both groups of children recruited frontal and parietal cortical areas that overlapped with areas indicated in the meta-analysis of n-back studies in children (Yaple & Arsalidou, 2018). The EPB group, however, showed fewer clusters of activation with a left hemispheric dominance, particularly in the cognitively demanding 2-back task. When the memory load increased from 1-back to 2-back, the TB children increased activation in the right SFG and MFG in regions that have been related to maintenance and manipulation of information in WM (Crone, Wendelken, Donohue, van Leijenhorst, & Bunge, 2006) and to the development of visuospatial WM capacity (Klingberg, 2006; Klingberg, Forssberg, & Westerberg., 2002). The EPB children failed to increase activation in any brain areas when memory load increased from 1-back to 2-back. These within-group analyses showed that TB children were able to recruit additional processing resources during the 2-back task compared to 1-back task, whereas EPB children had used their available processing resources already in the lower load level. Moreover, the weaker brain activations in EPB children were not sufficient to meet the task demands. Their performance was poorer than in the control group during the n-back tasks, and in the 2-back task it was associated with lower level of activation in the left PFCdl and PFCmed.

Between-group comparisons showed significantly enhanced prefrontal activation in TB than EPB children, especially in the right FP and OFC during attention and WM tasks. These regions have been indicated in executive control of goal-directed behavior (Mansouri, Koechlin, Rosa, & Buckley, 2017), monitoring and manipulation of subgoals maintained in WM (Braver & Bongiolatti, 2002) and cognitive control processes (Levy & Wagner, 2011). Earlier, Griffiths et al. (2013, 2014) performed fMRI on 11-year-old extremely prematurely-born children while they performed a combined Stroop n-back task. In line with the present study, they reported reduced activation in the preterm compared with term-born children in the prefrontal cortical areas and, in addition, in parietal areas. Another fMRI study, investigating 7-12-year-old very preterm-born children performing a dot-location WM task, found weaker activation in the right MFG and, using a ROI analysis, stronger activation in bilateral SFG in the preterm compared with control children (Mürner-Lavanchy et al., 2014). Recently, 13-year-old very preterm-born children performing visuospatial WM tasks, were also reported to activate more the bilateral SFG and left MFG (Arthursson et al., 2017), whereas a preliminary fMRI study in 7-9-year-old very preterm children found no frontal activations during 0- and 1-back tasks, but reported reduced activation in medial parietal and temporal regions, when compared with controls (Taylor et al., 2012). The discrepancies between the results of these earlier studies are not easily explained but may at least partially be due to the different age ranges of the participating subjects, variability in the extent of prematurity, and to differences in the applied tasks. The finding of the current study that EPB children performed the tasks with lower accuracy and activated WM-related brain areas less than the term-born controls, suggests that visuospatial WM in the EPB children is less developed than in their age-matched controls.

During WM tasks, EPB children appeared to activate the right temporal lobe areas more than TB children (Fig. 3D). However, Fig. 3E shows that both groups of children deactivated

this area during 1-back and 2-back tasks. The TB children deactivated this region more than EPB children resulting in stronger “activation” of the right temporal lobe areas in the EPB > TB comparison. The voxels that were differentially activated between the groups included areas in the right TP, Hipp and PHG (Supplementary Table 3). A longitudinal study in typically developing adolescents performing a delayed match-to-sample letter task found that the Hipp is involved in WM during early but not late adolescence (Finn et al., 2010) suggesting that its role in WM diminishes over maturation. Our finding that both groups deactivated the right temporal lobe areas shows, on one hand, that these structures are not involved in visuospatial WM processing in 7.5-year-old children and, on the other hand, that EPB compared with TB children exhibit poorer control over task-negative areas. Deactivation of medial temporal lobe structures (hippocampus) during n-back tasks has been demonstrated in adults (Cousijn, Rijpkema, Qin, van Wingen, & Fernández, 2012). Deactivation of task-irrelevant brain areas has been suggested to increase efficiency of task-activated networks (Tomasi, Ernst, Caparelli, & Chang, 2006) thereby supporting performance of cognitively demanding tasks. The downregulation of the right temporal lobe areas in term-born controls may represent a neural support mechanism for WM function resulting in better performance.

#### *4.2. Group differences in white matter microstructure*

Development of WM capacity has been associated with the maturation of the white matter especially in neural tracts connecting the fronto-parietal regions (Darki & Klingberg 2015; Nagy et al., 2004; Olesen et al., 2003; Vestergaard et al., 2011;). Since EPB children performed the tasks with lower accuracy and activated WM-related areas less than controls, we expected to find lower FA in EPB than TB children. We, however, found significantly higher FA values and decreased diffusivities in EPB children i.a. in SLF and IFO/ILF that enable complex sensorimotor and cognitive functions. Tracts in the SLF link superior and medial parietal regions with supplementary and premotor frontal areas, parieto-occipital areas

with dorsolateral prefrontal cortex, and inferior parietal regions with ventral prefrontal areas (Schmahmann, Smith, Eichler, & Filley, 2008). These pathways are involved in multiple cognitive functions including higher motor control, visuospatial attention, WM and language processing. The ILF is part of the ventral visual system forming connections between the occipital and temporal cortices (Catani, Jones, Donato & Ffytche, 2003) and IFO between occipital and frontal areas (Wu, Sun, Wang, & Wang, 2016) supporting visual associative processes, object recognition and memory.

Our findings of increased FA and decreased diffusivities in EPB children differ from a number of previous studies that reported reduced FA in multiple white matter regions in preterm-born compared with term-born subjects (Eikenes et al., 2011; Li et al., 2015; Skranes et al., 2007; Vangberg et al., 2006; Vollmer et al., 2017). However, several earlier studies on prematurely born infants, children and adults have also reported higher FA compared with controls (Allin et al., 2011; Gimenez et al., 2008; Feldman et al., 2012). Moreover, studies on neurodevelopmental disorders have also found increased FA in subjects diagnosed with ADHD (Li et al., 2010; Silk, Vance, Rinehart, Bradshaw, & Cunnington, 2009; Svatkova et al., 2016), autism (Weinstein et al., 2011) or Williams syndrome (Hoeft et al., 2007). In some of these studies, higher FA was linked with poorer neurobehavioral status and more severe symptoms (Hoeft et al., 2007; Svatkova et al., 2016).

The cellular mechanisms underlying increased FA in EPB children are unclear. The DTI-based parameters measure white-matter properties only indirectly and are affected by several factors including myelination of axons, and axonal diameter and density (Beaulieu, 2002). An elevated FA could be attributed to increased fiber density, higher degree of myelination or fiber organization (Li et al., 2010), and fewer but larger axons (Dougherty et al., 2007). In clinical populations, microscopic structural deficits in axons, changes in axonal diameter, packing density, and branching may contribute to higher FA (Beaulieu, 2002; Hoeft et al.,

2007). Moreover, several lines of evidence suggest that activity along axons influences myelination (reviewed by Sampaio-Baptista & Johansen-Berg, 2017) and that training and learning can increase FA (Scholz, Klein, Behrens, & Johansen-Berg, 2009). Reduced FA, on the other hand, can be observed in regions of crossing fibers where axons are less organized and less aligned along the same axis (Jones, Knösche, & Turner, 2013). Accordingly, there are several possible explanations for the current results. Extremely premature birth may trigger abnormal cellular mechanisms that affect the white matter integrity and development. It is also possible that EPB children, compared with term-born peers, have needed more effort and training to achieve different motor and cognitive skills that may have impeded development of the white matter, resulting in higher FA and lower diffusivities. Longitudinal studies that measure both brain structure and function are needed to better understand the relationships between premature birth, brain development and development of cognitive abilities.

In terms of DTI, the FA characterizes the shape of diffusion tensor ellipsoid, whose major eigenvalue (AD) reflects the diffusion along the axonal length, and an average of two minor eigenvalues (RD) diffusion perpendicular to the axonal wall (Aung, Mar, & Benzinger, 2013). Therefore, an increase in FA could be driven by enhanced AD, restricted RD or by their combination defined by MD. The MD describes an overall diffusion within the tissue while the RD is selectively sensitive to myelination of axons. In our study, the EPB compared with TB children, demonstrated decreased RD and MD in several white matter regions where FA was increased including bilateral SLF, IFO/ILF, CST, and CC, and reduced AD in anterior thalamic radiation and left ILF. Together these results suggest that increased FA in EPB children might be driven mainly by reduced RD reflecting the level of myelination (Song et al., 2005), and to a lesser extent by lower AD that is associated with the size of axonal caliber or packing of the tracts. Further studies using multicompartiment models such as NODDI

(neurite orientation dispersion and density imaging) (Zhang et al., 2012) would produce more specific information about neurobiological properties of the white matter changes. Such models require that the data are acquired using several sets of encoding directions with higher diffusion strength ( $>1000$  s/mm<sup>2</sup>), whereas our protocol was specifically designed for pediatric studies and used lower b-values, considering the higher water content in the developing brain structures (Sundgren et al., 2004).

#### *4.3. Associations of white matter microstructure with WM task performance speed*

The TBSS analysis showed significant associations between DTI parameters and WM performance in the TB group. TB children with higher FA and lower MD or RD in a widespread network of white matter regions had faster RTs during WM tasks. The regions with correlated FA values were in the bilateral IFO/ILF, SLF and CST. The regions with correlated MD values were in the right SLF and ILF, and those with correlated RD values in the right SLF, IFO, CC, CST and anterior thalamic radiation. The correlations between the DTI measures and response speed in TB children reported here are in accordance with several previous studies that also found associations between the white matter microstructure and processing speed in visuospatial learning (Tuch et al., 2005), visuomotor (Madsen et al., 2011; Scantlebury et al., 2014) and visual perceptual WM (Sala-Llonch, Palacios, Junqué, Bargallo, & Vendrell, 2015) tasks. EPB children demonstrated no significant correlations between the DTI parameters and processing speed, although they had higher FA and lower diffusivity, which are usually considered to be positive signs of neurodevelopment (Barnea-Golary et al., 2005; Cascio et al., 2007), and performed the tasks faster than the TB children, albeit at the expense of accuracy. This lack of correlations between performance speed and DTI measures in EPB children suggests that they did not benefit from the changes in the white matter microstructure.

#### *4.4. Associations of white matter microstructure with neuropsychological test scores*

The TB children demonstrated positive associations of MD, RD and AD with the number of inhibitory errors in the visual attention test suggesting that the lower the diffusivity the better the performance. Significant associations were observed in bilateral SLF, IFO/ILF, CC, CST and anterior thalamic radiation. These long-range association tracts mediate the processing of visual information and attention and the developmental state of these tracts affects information processing within regions of dorsal and ventral attention networks. These results suggest that in typically-developing children, lower diffusivities in structural connections that mediate information flow among frontal and parietal regions result in better performance in tasks requiring visual attention.

In EPB children, visuospatial test scores correlated negatively with FA values in the right posterior cerebellum indicating that children with lower FA values scored better. Earlier, the cerebellum was primarily related to motor functions (Ito, 2002), but more recently its role in higher cognitive processes has been acknowledged (E, Chen, Ho, & Desmond, 2014; Klein, Ulmer, Quinet, Mathews, & Mark, 2016). The white matter area in the cerebellum (VI/Crus I) that in EPB children exhibited associations with visuospatial performance has structural connections with the prefrontal and posterior parietal cortices (Jissendi, Baudry, & Balériaux, 2008; Ramnani, 2006; Salmi et al., 2010), i.e. key areas in attention and WM. Developmental changes in the white matter include myelination of axons which is considered important for the development of cognitive functions during childhood (Nagy et al., 2004), and increases in FA have been attributed to better myelination or higher axonal density of the tracts (Beaulieu, 2002). The findings that higher FA values in the cerebellum in EPB children were linked with poorer visuospatial performance, and that EPB children overall had higher FA values than term-born controls in several white matter areas suggest that higher FA does not necessarily

indicate better performance, and that the development of the white matter microstructure in EPB children is altered compared to TB children.

#### *4.5. Limitations of the study*

The study has some limitations. First, the number of subjects was relatively low due to strict inclusion criteria as we aimed to recruit EPB children with no major MRI abnormalities at term equivalent age, no neurological disorders or diagnosed cognitive deficiencies. EPB children did not differ significantly from the TB children in neuropsychological tests measuring visual attention and visual memory skills but they had lower scores in a subtest measuring Performance IQ (Matrix Reasoning) and in tests of visuospatial processing (Arrows and Block construction tests). Their age-scaled scores in these tests were still within normal range. However, the between-group differences in brain activation patterns, and DTI parameters, and associations between brain measures and behavior, were large enough to come up also in this sample size. Second, the maternal education of EPB children was lower than that of TB children. This parameter is difficult to control as children from families with higher education or socioeconomic background tend to participate in these kinds of studies more often than children from lower socioeconomic background (Aronen et al., 2005; Vuontela et al., 2013). Third, we applied TBSS analysis on DTI data to evaluate white matter organization. The DTI-based parameters are quite sensitive to microstructural changes, however, it remains challenging to make inferences about the underlying neuroanatomical properties and the results must be interpreted with caution. Moreover, TBSS fails to determine changes in regions of crossing fibers that constitute a great portion of the fiber population. Nevertheless, the TBSS approach remains a reliable exploratory tool for the evaluation of whole-brain structural changes (Kuhn et al., 2016). Finally, the EPB children had no or only mild abnormalities in the MRIs at term-age (Supplementary Table 1). However, the MRIs at age 7.5-y did not undergo a comparable detailed evaluation, and we did

not perform volumetric measurements of the brain structures. Thus, we cannot exclude the possibility that some structural group differences might have contributed to the microstructural findings of the white matter reported here. Follow-up studies are needed to better understand the observed differences in the white matter microstructure between school-aged preterm-born and control children.

## **5. Conclusions**

Functional MRI and DTI were performed in high-functioning 7.5-year-old children born extremely prematurely, and in age-matched controls born at term. The preterm-born children, compared with controls, performed attention and WM tasks with lower accuracy, and had reduced brain activation during the tasks. In prefrontal cortical areas, the lower level of activation correlated with poorer task performance. Moreover, DTI suggested higher anisotropy and lower diffusivity in several white matter tracts in preterm-born children. However, they did not seem to benefit from these microstructural changes as higher anisotropy and lower diffusivity associated with faster performance and better neuropsychological scores only in control children. The demonstration of altered brain functions and white matter microstructure in the extremely prematurely born children, who had normal global cognitive ability, is alerting since these children usually enter normal schools and are expected to perform as well as others. The current study provides a view to brain responsiveness, white matter microstructure and cognitive performance at a narrow time-point when the children had just started formal school education. Longitudinal studies applying both functional and structural brain imaging are needed to better understand the neural mechanisms underlying these findings and their long-term effects on cognitive and behavioral development.

## **Acknowledgements**

We wish to thank Dr. Carlo Pierpaoli for his suggestions and help in designing the protocols and handling of the DTI data, Dr. Taina Autti and Dr. Leena Valanne for classifying the neonatal brain magnetic resonance images, Marita Kattelus for her invaluable help in brain imaging and Dr. Suvi Viskari-Lähdeoja for ophthalmological examinations of the children.

## **Funding**

This work was supported by grants from Academy of Finland (grant numbers 259752, 273147 to S.C.), Päivikki and Sakari Sohlberg Foundation (S.C.), Aalto Brain Centre (S.C.), University of Helsinki (375th Anniversary grant to S.C.); Foundation for Pediatric Research (M.M., P.L., S.A.), Hospital District of Helsinki and Uusimaa Medical Imaging Centre (J.P.), Finnish Cultural Foundation (M.T.), Instrumentarium Science Foundation (M.T.), Arvo and Lea Ylppö Foundation (A.L., P.L.), The Finnish Medical Foundation (P.L.), Finska Läkaresällskapet (S.A.), Governmental Subsidy for Clinical Research (S.A.), Helsinki University Central Hospital Research Funds (TYH 2014104 to A.L., and TYH 2016202 and TYH 2017205 to V.V.) and Yrjö Jahnsson Foundation (V.V).

## **References**

- Aarnoudse-Moens, C.S., Weisglas-Kuperus, N., van Goudoever, J.B., & Oosterlaan, J. (2009). Meta-analysis of neurobehavioral outcomes in very preterm and/or very low birth weight children. *Pediatrics*, 124, 717-728.
- Allin, M.P., Kontis, D., Walshe, M., Wyatt, J., Barker, G.J., Kanaan, R.A., McGuire, P., Rifkin, L., Murray, R.M., & Nosarti, C. (2011). White matter and cognition in adults who were born preterm. *PLoS One*, 6(10), e24525.

- Alloway, T.P., & Alloway, R.G. (2010). Investigating the predictive roles of working memory and IQ in academic attainment. *Journal of Experimental Child Psychology*, 106, 20-29.
- Aronen, E.T., Vuontela, V., Steenari, M.R., Salmi, J., & Carlson, S. (2005). Working memory, psychiatric symptoms, and academic performance at school. *Neurobiology of Learning and Memory*, 83, 33-42.
- Arthursson, P.M., Thompson, D.K., Spencer-Smith, M., Chen, J., Silk, T., Doyle, L.W., & Anderson, P.J. (2017). Atypical neuronal activation during a spatial working memory task in 13-year-old very preterm children. *Human Brain Mapping*, 38, 6172-6184.
- Aung, W.Y., Mar, S., & Benzinger, T.L. (2013). Diffusion tensor MRI as a biomarker in axonal and myelin damage. *Imaging in Medicine*, 5(5), 427-440.
- Bach, M., Laun, F.B., Leemans, A., Tax, C.M., Biessels, G.J., Stieltjes, B., & Maier-Hein, K.H. (2014). Methodological considerations on tract-based spatial statistics (TBSS). *Neuroimage*, 100, 358-69.
- Baldoli, C., Scola, E., Della Rosa, P.A., Pontesilli, S., Longaretti, R., Poloniato, A., Scotti, R., Blasi, V., Cirillo, S., Iadanza, A., Rovelli, R., Barera, G., & Scifo, P. (2015). Maturation of preterm newborn brains: a fMRI-DTI study of auditory processing of linguistic stimuli and white matter development. *Brain Structure and Function*, 220, 3733-3751.
- Barnea-Golary, N., Menon, V., Eckert, M., Tamm, L., Bammer, R., Karchemskiy, A., Dant, C.C., & Reiss, A.I. (2005). White matter development during childhood and adolescence: A cross-sectional diffusion tensor imaging study. *Cerebral Cortex*, 15, 1848-1854.
- Beaulieu, C. (2002). The basis of anisotropic water diffusion in the nervous system - a technical review. *NMR in Biomedicine*, 15(7-8), 435-55.
- Beckmann, C.F., Jenkinson, M., & Smith, S.M. (2003). General multilevel linear modeling for group analysis in FMRI. *Neuroimage*, 20, 1052-1063.

- Braver, T.S., & Bongiolatti, S.R. (2002). The role of frontopolar cortex in subgoal processing during working memory. *Neuroimage*, 15,523-536.
- Burnett, A.C., Anderson, P.J., Lee, K.J., Roberts, G., Doyle, L.W., & Cheong, J.L. (2018). Trends in executive functioning in extremely preterm children across 3 birth eras. *Pediatrics*, 141(1), e20171958.
- Burnett, A.C., Scratch, S.E., & Anderson, P.J. (2013). Executive function outcome in preterm adolescents. *Early Human Development*, 89, 215-220.
- Cascio, C.J., Gerig, G., & Piven, J. (2007). Diffusion tensor imaging: application to the study of the developing brain. *Journal of the American Academy of Child and Adolescent Psychiatry*, 46, 213–223.
- Catani, M., Jones, D.K., Donato, R., & Ffytche, D.H. (2003). Occipito-temporal connections in the human brain. *Brain*, 126(Pt 9), 2093-107.
- Chang, L.C., Jones, D.K., & Pierpaoli, C. (2005). RESTORE: robust estimation of tensors by outlier rejection. *Magnetic Resonance in Medicine*, 53, 1088-1095.
- Cheong, J.L., Anderson, P.J., Burnett, A.C., Roberts, G., Davis, N., Hickey, L., Carse, E., & Doyle, L.W. (2017). Changing neurodevelopment at 8 years in children born extremely preterm since the 1990s. *Pediatrics*, 139(6), e2014086.
- Clark, C.A., & Woodward, L.J. (2010). Neonatal cerebral abnormalities and later verbal and visuospatial working memory abilities of children born very preterm. *Developmental Neuropsychology*, 35, 622-642.
- Cousijn, H., Rijpkema, M., Qin, S., van Wingen, G.A., & Fernández, G. (2012). Phasic deactivation of the medial temporal lobe enables working memory processing under stress. *Neuroimage*, 59, 1161-1167.

- Crone, E.A., Wendelken, C., Donohue, S., van Leijenhorst, L., & Bunge, S.A. (2006). Neurocognitive development of the ability to manipulate information in working memory. *Proceedings of the National Academy of Sciences of the United States of America*, 103, 9315-9320.
- Cui, J., Tymofiyeva, O., Desikan, R., Flynn, T., Kim, H., Gano, D., Hess, C.P., Ferriero, D.M., Barkovich, A.J., & Xu, D. (2017). Microstructure of the default mode network in preterm infants. *American Journal of Neuroradiology*, 38, 343-348.
- Daamen, M., Bäuml, J.G., Scheef, L., Sorg, C., Busch, B., Baumann, N., Bartmann, P., Wolke, D., Wohlschläger, A., & Boecker, H. (2015). Working memory in preterm-born adults: load-dependent compensatory activity of the posterior default mode network. *Human Brain Mapping*, 36, 1121-1137.
- Darki, F., & Klingberg, T. (2015). The role of fronto-parietal and fronto-striatal networks in the development of working memory: A longitudinal study. *Cerebral Cortex*, 25, 1587-1595.
- Dempster, F.N. (1992). The rise and fall of the inhibitory mechanism: Toward a unified theory of cognitive development and aging. *Developmental Review*, 12, 45-75.
- Dougherty, R.F., Ben-Shachar, M., Deutsch, G.K., Hernandez, A., Fox, G.R., & Wandell, B.A. (2007). Temporal-callosal pathway diffusivity predicts phonological skills in children. *Proceedings of the National Academy of Sciences of the United States of America*, 104, 8556-61.
- Duerden, E.G., Card, D., Lax, I.D., Donner, E.J., & Taylor, M.J. (2013). Alterations in frontostriatal pathways in children born very preterm. *Developmental Medicine and Child Neurology*, 55(10), 952-958.

- E, K.H., Chen, S.H., Ho, M.H., & Desmond, J.E. (2014). A meta-analysis of cerebellar contributions to higher cognition from PET and fMRI studies. *Human Brain Mapping*, 35(2), 593-615.
- Eikenes, L., Løhaugen, G.C., Brubakk, A.M., Skranes, J., & Håberg, A.K. (2011). Young adults born preterm with very low birth weight demonstrate widespread white matter alterations on brain DTI. *Neuroimage*, 54(3), 1774-1785.
- Feldman, H.M., Lee, E.S., Loe, I.M., Yeom, K.W., Grill-Spector, K., & Luna, B. (2012). White matter microstructure on diffusion tensor imaging is associated with conventional magnetic resonance imaging findings and cognitive function in adolescents born preterm. *Developmental Medicine and Child Neurology*, 54(9), 809-14.
- Finn, A.S., Sheridan, M.A., Kam, C.L., Hinshaw, S., & D'Esposito, M. (2010). Longitudinal evidence for functional specialization of the neural circuit supporting working memory in the human brain. *Journal of Neuroscience*, 30, 11062-11067.
- Gimenez, M., Miranda, M.J., Born, A.P., Nagy, Z., Rostrup, E., & Jernigan, T.L. (2008). Accelerated cerebral white matter development in preterm infants: a voxel-based morphometry study with diffusion tensor MR imaging. *Neuroimage*, 41, 728-34.
- Griffiths, S.T., Aukland, S.M., Markestad, T., Eide, G.E., Elgen, I., Craven, A.R., & Hugdahl, K. (2014). Association between brain activation (fMRI), cognition and school performance in extremely preterm and term born children. *Scandinavian Journal of Psychology*, 55, 427-432.
- Griffiths, S.T., Gundersen, H., Neto, E., Elgen, I., Markestad, T., Aukland, S.M., & Hugdahl, K. (2013). fMRI: blood oxygen level-dependent activation during a working memory-selective attention task in children born extremely preterm. *Pediatric Research*, 74, 196-205.

- Hoefl, F., Barnea-Goraly, N., Haas, B.W., Golarai, G., Ng, D., Mills, D., Korenberg, J., Bellugi, U., Galaburda, A., & Reiss, A.I. (2007). More is not always better: increased fractional anisotropy of superior longitudinal fasciculus associated with poor visuospatial abilities in Williams syndrome. *Journal of Neuroscience*, 27(44), 11960-11965.
- Hutchinson, E.A., De Luca, C.R., Doyle, L.W., Roberts, G., & Anderson, P.J. (2013). School-age outcomes of extremely preterm or extremely low birth weight children. *Pediatrics*, 131, e1053-e1061.
- Irfanoglu, M.O., Modi, P., Nayak, A., Hutchinson, E.B., Sarlls, J., & Pierpaoli, C. (2015). DR-BUDDI (Diffeomorphic Registration for Blip-Up blip-Down Diffusion Imaging) method for correcting echo planar imaging distortions. *Neuroimage*, 106, 284-299.
- Ito, M. (2002). Historical review of the significance of the cerebellum and the role of Purkinje cells in motor learning. *Annals of the New York Academy of Sciences*, 978, 273–288.
- Jenkinson, M., Bannister, P., Brady, M., & Smith, S. (2002). Improved optimization for the robust and accurate linear registration and motion correction of brain images. *Neuroimage*, 17, 825-841.
- Jenkinson, M., & Smith, S. (2001). A global optimization method for robust affine registration of brain images. *Medical Image Analysis*, 5, 143-156.
- Jissendi, P., Baudry, S., & Balériaux, D. (2008). Diffusion tensor imaging (DTI) and tractography of the cerebellar projections to prefrontal and posterior parietal cortices: a study at 3T. *Journal of Neuroradiology*, 35(1), 42-50.
- Johnson, S., Fawke, J., Hennessy, E., Rowell, V., Thomas, S., Wolke, D., & Marlow, N. (2009). Neurodevelopmental disability through 11 years of age in children born before 26 weeks of gestation. *Pediatrics*, 124, e249-e257.

- Jones, D.K., Knösche, T.R., & Turner, R. (2013). White matter integrity, fiber count, and other fallacies: The do's and don'ts of diffusion MRI. *Neuroimage*, 73, 239-254.
- Kalpakidou, A.K., Allin, M.P., Walshe, M., Giampietro, V., McGuire, P.K., Rifkin, L., Murray, R.M., & Nosarti, C. (2014). Functional neuroanatomy of executive function after neonatal brain injury in adults who were born very preterm. *PLoS One*, 9(12), e113975.
- Klein, A.P., Ulmer, J.L., Quinet, S.A., Mathews, V., & Mark, L.P. (2016). Nonmotor Functions of the Cerebellum: An Introduction. *American Journal of Neuroradiology*, 37(6), 1005-9.
- Klingberg, T. (2006). Development of a superior frontal-intraparietal network for visuospatial working memory. *Neuropsychologia*, 44, 2171-77.
- Klingberg, T., Forssberg, H., & Westerberg, H. (2002). Increased brain activity in frontal and parietal cortex underlies the development of visuospatial working memory capacity during childhood. *Journal of Cognitive Neuroscience*, 14, 1-10.
- Koivisto, A., Klenberg, L., Tommiska, V., Lano, A., Laine, M., Fellman, V., & Haavisto, A. (2015). Parents tend to underestimate cognitive deficits in 10- to 13-year-olds born with an extremely low birth weight. *Acta Paediatrica*, 104, 1182-1188.
- Korkman, M., Kirk, U., & Kemp S editors. NEPSY-II - Lasten neuropsykologinen tutkimus. Psykologien kustannus; 2008.
- Kriegeskorte, N., Simmons, W.K., Bellgowan, P.S., & Baker, C.I. (2009). Circular analysis in systems neuroscience: the dangers of double dipping. *Nature Neuroscience*, 12, 535-540.
- Kuhn, T., Gullett, J.M., Nguyen, P., Boutzoukas, A.E., Ford, A., Colon-Perez, L.M., Triplett, W., Carney, P.R., Mareci, T.H., Price, C.C., & Bauer, R.M. (2016). Test-retest reliability of high angular resolution diffusion imaging acquisition within medial temporal lobe

- connections assessed via tract based spatial statistics, probabilistic tractography and a novel graph theory metric. *Brain Imaging and Behavior*, 10(2), 533-47.
- Levy, B.J., & Wagner, A.D. (2011). Cognitive control and right ventrolateral prefrontal cortex: reflexive reorienting, motor inhibition, and action updating. *Annals of the New York Academy of Sciences*, 1224, 40-62.
- Li, Q., Sun, J., Guo, L., Zang, Y., Feng, Z., Huang, X., Yang, H., Lv, Y., Huang, M., & Gong, Q. (2010). Increased fractional anisotropy in white matter of the right frontal region in children with attention-deficit/hyperactivity disorder: A diffusion tensor imaging study. *Activitas Nervosa Superior Rediviva*, 52(3), 193–199.
- Li, K., Sun, Z., Han, Y., Gao, L., Yuan, L., & Zeng, D. (2015). Fractional anisotropy alterations in individuals born preterm: a diffusion tensor imaging meta-analysis. *Developmental Medicine & Child Neurology*, 57, 328-338.
- Lieberman, M.D., & Cunningham, W.A. (2009). Type I and Type II error concerns in fMRI research: re-balancing the scale. *Social Cognitive and Affective Neuroscience*, 4, 423-428.
- Loe, I.M., Lee, E.S., & Feldman, H.M. (2013). Attention and internalizing behaviors in relation to white matter in children born preterm. *Journal of Developmental & Behavioral Pediatrics*, 34(3), 156-164.
- Luu, T.M., Ment, L., Allan, W., Schneider, K., & Vohr, B.R. (2011). Executive and memory function in adolescents born very preterm. *Pediatrics*, 127, e639-e646.
- Madsen, K.S., Baaré, W.F., Skimminge, A., Vestergaard, M., Siebner, H.R., & Jernigan, T.L. (2011). Brain microstructural correlates of visuospatial choice reaction time in children. *Neuroimage*, 58(4), 1090-100.

- Mansouri, F.A., Koechlin, E., Rosa, M.G., & Buckley, M.J. (2017). Managing competing goals – a key role for the frontopolar cortex. *Nature Reviews Neuroscience*, 18(11), 645-657.
- Mulder, H., Pitchford, N.J., & Marlow, N. (2010). Processing speed and working memory underlie academic attainment in very preterm children. *Archives of Disease in Childhood Fetal and Neonatal Ed*, 95, F267-F272.
- Mürner-Lavanchy, I., Ritter, B.C., Spencer-Smith, M.M., Perrig, W.J., Schroth, G., Steinlin, M., & Everts, R. (2014). Visuospatial working memory in very preterm and term born children—Impact of age and performance. *Developmental Cognitive Neuroscience*, 9, 106-116.
- Murray, A.L., Thompson, D.K., Pascoe, L., Leemans, A., Inder, T.E., Doyle, L.W., Anderson, J.F., & Anderson, P.J. (2016). White matter abnormalities and impaired attention abilities in children born very preterm. *Neuroimage*, 124, 75-84.
- Nagy, Z., Westerberg, H., & Klingberg, T. (2004). Maturation of white matter is associated with the development of cognitive functions during childhood. *Journal of Cognitive Neuroscience*, 16, 1227-1233.
- Narberhaus, A., Lawrence, E., Allin, M.P., Walshe, M., McGuire, P., Rifkin, L., Murray, R., & Nosarti, C. (2009). Neural substrates of visual paired associates in young adults with a history of very preterm birth: Alterations in fronto-parieto-occipital networks and caudate nucleus. *Neuroimage*, 47, 1884-1893.
- Nosarti, C., Shergill, S.S., Allin, M.P., Walshe, M., Rifkin, L., Murray, R.M., & McGuire, P.K. (2009). Neural substrates of letter fluency processing in young adults who were born very preterm: alterations in frontal and striatal regions. *Neuroimage*, 47(4), 1904-1913.

- O'Brien, F., Roth, S., Stewart, A., Rifkin, L., Rushe, T., & Wyatt, J. (2004). The neurodevelopmental progress of infants less than 33 weeks into adolescence. *Archives of Disease in Childhood*, 89, 207-211.
- Olesen, P.J., Nagy, Z., Westerberg, H., & Klingberg, T. (2003). Combined analysis of DTI and fMRI data reveals a joint maturation of white and grey matter in fronto-parietal network. *Cognitive Brain Research*, 18, 48-57.
- Omizzolo, C., Scratch, S.E., Stargatt, R., Kidokoro, H., Thompson, D.K., Lee, K.J., Cheong, J., Neil, J., Inder, T.E., Doyle, L.W., & Anderson, P.J. (2013). Neonatal brain abnormalities and memory and learning outcomes at 7 years in children born very preterm. *Memory*, 22, 605-615.
- Owen, A.M., McMillan, K.M., Laird, A.R., & Bullmore, E. (2005). N-back working memory paradigm: A meta-analysis of normative functional imaging studies. *Human Brain Mapping*, 25, 46-59.
- Pierpaoli, C., Walker, L., Irfanoglu, M.O., Barnett, A., Basser, P., Chang, L-C., Koay, C., Pajevic, S., Rohde, G., Sarlls, J., & Wu, M. (2010). TORTOISE: an integrated software package for processing of diffusion MRI data. ISMRM 18th annual meeting 2010, Stockholm, Sweden, #1597.
- Rahkonen, P., Heinonen, K., Pesonen, A.K., Lano, A., Autti, T., Puosi, R., Huhtala, E., Andersson, S., Metsäranta, M., & Räikkönen, K. (2014). Mother-child interaction is associated with neurocognitive outcome in extremely low gestational age children. *Scandinavian Journal of Psychology*, 55,311-318.
- Rahkonen, P., Nevalainen, P., Lauronen, L., Pihko, E., Lano, A., Vanhatalo, S., Pesonen, A.K., Heinonen, K., Räikkönen, K., Valanne, L., Autti, T., Andersson, S., & Metsäranta, M. (2013). Cortical somatosensory processing measured by magnetoencephalography

- predicts neurodevelopment in extremely low-gestational-age infants. *Pediatric Research*, 73, 763-771.
- Ramnani, N. (2006). The primate cortico-cerebellar system: anatomy and function. *Nature Reviews Neuroscience*, 7(7), 511-522.
- Saavalainen, P., Luoma, L., Bowler, D., Määttä, S., Kiviniemi, V., Laukkanen, E., & Herrgård, E. (2007). Spatial span in very prematurely born adolescents. *Developmental Neuropsychology*, 32, 769-785.
- Sala-Llonch, R., Palacios, E.M., Junqué Bargallo, N., & Vendrell, P. (2015). Functional networks and structural connectivity of visuospatial and visuo-perceptual working memory. *Frontiers in Human Neuroscience*, 9, 340.
- Salmi, J., Pallesen, K.J., Neuvonen, T., Brattico, E., Korvenoja, A., Salonen, O., & Carlson, S. (2010). Cognitive and motor loops of the human cerebro-cerebellar system. *Journal of Cognitive Neuroscience*, 22(11), 2663-76.
- Salvan, P., Walsh, S.F., Allin, M.P., Walshe, M., Murray, R.M., Bhattacharyya, S., McGuire, P.K., Williams, S.C., & Nosarti, C. (2014). Road work on memory lane – Functional and structural alterations to the learning and memory circuit in adults born very preterm. *Neuroimage*, 102 (Pt 1), 152-161.
- Sampaio-Baptista, C., & Johansen-Berg, H. (2017). White matter plasticity in the adult brain. *Neuron*, 96(6), 1239-1251.
- Scantlebury, N., Cunningham, T., Dockstader, C., Laughlin, S., Gaetz, W., Rockel, C., Dickson, J., & Mabbott, D. (2014). Relations between white matter maturation and reaction time in childhood. *Journal of the International Neuropsychological Society*, 20(1), 99-112.

- Schmahmann, J.D., Smith, E.E., Eichler, F.S., & Filley, C.M. (2008). Cerebral white matter: neuroanatomy, clinical neurology, and neurobehavioral correlates. *Annals of the New York Academy of Sciences*, 1142, 266-309.
- Scholz, J., Klein, M., Behrens, T., & Johansen-Berg, H. (2009). Training induces changes in white-matter architecture. *Nature Neuroscience*, 12, 1370–1371.
- Seaton, S.E., King, S., Manktelow, B.N., Draper, E.S., & Field, D.J. (2013). Babies born at the threshold of viability: changes in survival and workload over 20 years. *Archives of Disease in Childhood Fetal Neonatal Ed*, 98, F15–F20.
- Serenius, F., Ewald, U., Farooqi, A., Fellman, V., Hafström, M., Hellgren, K., Maršál, K., Ohlin, A., Olhager, E., Stjernqvist, K., Strömberg, B., Ådén, U., & Källén, K. (2016). Neurodevelopmental outcomes among extremely preterm infants 6.5 years after active perinatal care in Sweden. *JAMA Pediatrics*, 170, 954-963.
- Serenius, F., Källén, K., Blennow, M., Ewald, U., Fellman, V., Holmström, G., Lindberg, E., Lundqvist, P., Maršál, K., Norman, M., Olhager, E., Stigson, L., Stjernqvist, K., Vollmer, B., & Strömberg, B. (2013). Neurodevelopmental outcome in extremely preterm infants at 2.5 years after active perinatal care in Sweden. *JAMA*, 309, 1810-1820.
- Silk, T.J., Vance, A., Rinehart, N., Bradshaw, J.L., & Cunnington, R. (2009). White-matter abnormalities in attention deficit hyperactivity disorder: a diffusion tensor imaging study. *Human Brain Mapping*, 30(9), 2757-65.
- Skranes, J., Lohaugen, G.C., Martinussen, M., Indredavik, M.S., Dale, A.M., Haraldseth, O., Vangberg, T.R., & Brubakk, A-M. (2009). White matter abnormalities and executive function in children with very low birth weight. *NeuroReport*, 20, 263-266.
- Skranes, J., Vangberg, T.R., Kulseng, S., Indredavik, M.S., Evensen, K.A., Martinussen, M., Dale, A.M., Haraldseth, O., & Brubakk, A-M. (2007). Clinical findings and white matter

- abnormalities seen on diffusion tensor imaging in adolescents with very low birth weight. *Brain*, 130(Pt 3), 654-666.
- Smith, S.M., Jenkinson, M., Johansen-Berg, H., Rueckert, D., Nichols, T.E., Mackay, C.E., Watkins, K.E., Ciccarelli, O., Cader, M.Z., Matthews, P.M., & Behrens, T.E. (2006). Tract-based spatial statistics: voxelwise analysis of multi-subject diffusion data. *Neuroimage*, 31(4), 1487-1505.
- Song, S.K., Yoshino, J., Le, T.Q., Lin, S.J., Sun, S.W., Cross, A.H., & Armstrong, R.C. (2005). Demyelination increases radial diffusivity in corpus callosum of mouse brain. *Neuroimage*, 26(1), 132-40.
- Sundgren, P.C., Dong, Q., Gómez-Hassan, D., Mukherji, S.K., Maly, P., & Welsh, R. (2004). Diffusion tensor imaging of the brain: review of clinical applications. *Neuroradiology*, 46(5), 339-50.
- Svatkova, A., Nestrasil, I., Rudser, K., Goldenring Fine, J., Bledsoe, J., & Semrud-Clikeman, M. (2016). Unique white matter microstructural patterns in ADHD presentations-a diffusion tensor imaging study. *Human Brain Mapping*, 37(9), 3323-36.
- Taylor, H.G., & Clark, C.A. (2016). Executive function in children born preterm: Risk factors and implications for outcome. *Seminars in Perinatology*, 40(8), 520-529.
- Taylor, M.J., Donner, E.J., & Pang, E.W. (2012). fMRI and MEG in the study of typical and atypical cognitive development. *Clinical Neurophysiology*, 42, 19-25.
- Taylor, H.G., Klein, N., Minich, N.M., & Hack, M. (2000). Middle-school-age outcomes in children with very low birthweight. *Child Development*, 71, 1495-1511.
- Thompson, D.K., Chen, J., Beare, R., Adamson, C.L., Ellis, R., Ahmadzai, Z.M., Kelly, C.E., Lee, K.J., Zalesky, A., Yang, J.Y., Hunt, R.W., Cheong, J.L., Inder, T.E., Doyle, L.W.,

- Seal, M.L., & Anderson, P.J. (2016). Structural connectivity relates to perinatal factors and functional impairment at 7 years in children born very preterm. *Neuroimage*, 134, 328-337.
- Tomasi, D., Ernst, T., Caparelli, E.C., & Chang, L. (2006). Common deactivation patterns during working memory and visual attention tasks: An intra-subject fMRI study at 4 Tesla. *Human Brain Mapping*, 27(8), 694–705.
- Tuch, D.S., Salat, D.H., Wisco, J.J., Zaleta, A.K., Hevelone, N.D., & Rosas, H.D. (2005). Choice reaction time performance correlates with diffusion anisotropy in white matter pathways supporting visuospatial attention. *Proceedings of the National Academy of Sciences of the United States of America*, 102(34), 12212-12217.
- van den Heuvel, M.P., Kersbergen, K.J., de Reus, M.A., Keunen, K., Kahn, R.S., Groenendaal, F., de Vries, L.S., & Benders, M.J. (2015). The neonatal connectome during preterm brain development. *Cerebral Cortex*, 25, 3000-3013.
- Vangberg, T.R., Skranes, J., Dale, A.M., Martinussen, M., Brubakk, A.M., & Haraldseth, O. (2006). Changes in white matter diffusion anisotropy in adolescents born prematurely. *Neuroimage*, 32(4), 1538-1548.
- Vestergaard, M., Madsen, K.S., Baaré, W.F., Skimminge, A., Ejersbo, L.R., Ramsøy, T.Z., Gerlach, C., Åkeson, P., Paulson, O.B., & Jernigan, T.L. (2011). White matter microstructure in superior longitudinal fasciculus associated with spatial working memory performance in children. *Journal of Cognitive Neuroscience*, 23, 2135-2146.
- Vollmer, B., Lundequist, A., Mårtensson, G., Nagy, Z., Lagercrantz, H., Smedler, A.C., & Forssberg, H. (2017). Correlation between white matter microstructure and executive functions suggests early developmental influence on long fibre tracts in preterm born adolescents. *PLoS One*, 12, e0178893.

- Volpe, J.J. (2009). Brain injury in premature infants: a complex amalgam of destructive and developmental disturbances. *Lancet Neurology*, 8(1), 110-124.
- von Allmen, D.Y., Wurmitzer, K., & Klaver, P. (2014). Hippocampal and posterior parietal contributions to developmental increases in visual short-term memory capacity. *Cortex*, 59, 95-102.
- Vuontela, V., Jiang, P., Tokariev, M., Savolainen, P., Ma, Y.Y., Aronen, E.T., Fontell, T., Liiri, T., Ahlström, M., Salonen, O., & Carlson, S. (2013). Regulation of brain activity in the fusiform face and parahippocampal place areas in 7-11-year-old children. *Brain and Cognition*, 81, 203-214.
- Vuontela, V., Steenari, M.R., Carlson, S., Koivisto, J., Fjällberg, M., & Aronen, E.T. (2003). Audiospatial and visuospatial working memory in 6-13 year old school children. *Learning and Memory*, 10,74-81.
- Wang, H., He, W., Wu, J., Zhang, J., Jin, Z., & Li, L. (2019). A coordinate-based meta-analysis of the n-back working memory paradigm using activation likelihood estimation. *Brain and Cognition*, 132, 1-12.
- Wechsler, D., Heiskari, P., Jakobson, B., & Marila, A. (2009). Wechsler Preschool and Primary Scale of Intelligence – III Finnish Translation, Helsinki, Psykologien kustannus Oy.
- Weinstein, M., Ben-Sira, L., Levy, Y., Zachor, D.A., Ben Itzhak, E., Artzi, M., Tarrasch, R., Eksteine, P.M., Hendler, T., & Ben Bashat, D. (2011). Abnormal white matter integrity in young children with autism. *Human Brain Mapping*, 32(4), 534-43.
- Weinstein, M., Ben-Sira, L., Moran, A., Berger, I., Marom, R., Geva, R., Gross-Tsur, V., Leitner, Y., & Bashat, D.B. (2016). The motor and visual networks in preterm infants: An fMRI and DTI study. *Brain Research*, 1642, 603-611.

- Woodward, L.J., Anderson, P.J., Austin, N.C., Howard, K., & Inder, T.E. (2006). Neonatal MRI to predict neurodevelopmental outcomes in preterm infants. *New England Journal of Medicine*, 355, 685-694.
- Worsley, K.J., Evans, A.C., Marrett, S., & Neelin, P. (1992). A three-dimensional statistical analysis for CBF activation studies in human brain. *Journal of Cerebral Blood Flow & Metabolism*, 12, 900-918.
- Wu, Y., Sun, D., Wang, Y., & Wang, Y. (2016). Subcomponents and connectivity of the inferior fronto-occipital fasciculus revealed by diffusion spectrum imaging fiber tracking. *Frontiers in Neuroanatomy*, 10, 88.
- Yaple, Z., & Arsalidou, M. (2018). N-back working memory task: meta-analysis of normative fMRI studies with children. *Child Development*, 89, 2010–2022.
- Young, J.M., Vandewouw, M.M., Morgan, B.R., Smith, M.L., Sled, J.G., & Taylor, M.J. (2018). Altered white matter development in children born very preterm. *Brain Structure and Function*, 223, 2129–
- Zhang, H., Avants, B.B., Yushkevich, P.A., Woo, J.H., Wang, S., & McCluskey, L.H., et al. (2007). High-dimensional spatial normalization of diffusion tensor images improves the detection of white matter differences: an example study using amyotrophic lateral sclerosis. *IEEE Transactions on Medical Imaging*, 26, 1585-1597.
- Østby, Y., Tamnes, C.K., Fjell, A.M., & Walhovd, K.B. (2011). Morphometry and connectivity of the fronto-parietal verbal working memory network in development. *Neuropsychologia*, 49, 3854-3862.

**Table 1.** Descriptive characteristics of EPB and TB groups.

	EPB	TB	EPB vs. TB ( <i>P</i> )
<i>n</i>	16	16	
Males, <i>n</i> (%)	9 (56)	9 (56)	
Gestational age at birth, weeks, M (SD)	26.7 (0.8)	40.0 (0.9)	< 0.001**
Birth weight, g, M (SD)	866 (177)	3582 (433)	< 0.001**
Small for gestational age, <i>n</i> (%)	3 (19)	0 (0)	0.23
Twins, <i>n</i> (%)	7 (44)	0 (0)	0.007**
Bronchopulmonary dysplasia at 36 gwk, <i>n</i> (%)	7 (44)		
Necrotizing enterocolitis, <i>n</i> (%)	1 (6)		
Patent ductus arteriosus, <i>n</i> (%)	12 (75)		
Retinopathy of prematurity, <i>n</i> (%)	3 (19)		
Intraventricular hemorrhage in neonatal US, <i>n</i> (%)			
No	11 (69)		
Grade I	2 (13)		
Grade II	3 (19)		
Grade III/IV	0 (0)		
White matter injury in MRI at term age, <i>n</i> (%) <sup>a</sup>			
No	12 (75)		
Mild	4 (25)		
Moderate/Severe	0 (0)		
Age in fMRI/DTI, years, M (SD)	7.5 (0.1)	7.6 (0.2)	0.36
Right-handed, <i>n</i> (%)	13 (81)	14 (87.5)	1.0

Full scale IQ, M (SD) <sup>b</sup>	101 (8)	108 (13)	0.07
Performance IQ, M (SD) <sup>b</sup>	93 (12)	106 (17)	0.02*
Verbal IQ, M (SD) <sup>b</sup>	109 (9)	110 (12)	0.74
Visual attention, Visual attention test, M (SD) <sup>c</sup>	10 (1.8)	10.2 (2.1)	0.79
Visual memory, Memory for designs, M (SD) <sup>c</sup>	9.2 (2.4)	9.3 (2.2)	0.94
Visuospatial processing			
Arrows, M (SD) <sup>c</sup>	9.6 (1.7)	11.7 (1.9)	< 0.001**
Block construction, M (SD) <sup>c</sup>	9.1 (2.3)	11.6 (2.4)	0.004**
Maternal education, <i>n</i> (%)			0.003**
Secondary education	7 (44)	0 (0)	
Bachelor level	6 (38)	5 (31)	
Master level or higher	3 (19)	11 (69)	

---

\* $P < 0.05$ , \*\* $P < 0.01$  (Independent samples *t*-test, Fisher's Exact Test or Chi-square Test according to the variable type and expected frequency within cells). EPB, extremely prematurely-born; TB, term-born; gwk, gestational weeks; IQ, intelligence quotient; US, ultrasound.

<sup>a</sup> White matter injury classification according to Woodward, Anderson, Austin, Howard, & Inder, (2006). For a detailed description of the classification, see Supplementary Table 1.

<sup>b</sup> IQ by WPPSI-III (Wechsler et al., 2009).

<sup>c</sup> Visual attention, visual memory and visuospatial processing by Finnish edition of NEPSY-II (Korkman et al., 2008).

## Figure legends

**Figure 1** Flow-chart of the study groups.

A) Exclusion criteria: Grade III-IV intraventricular hemorrhage in neonatal cranial ultrasound (12 subj.), cerebral palsy (2 subj.), global cognitive impairment (FSIQ<85) (6 subj.), chromosomal abnormality (1 subj.), mutism (1 subj.), psychiatric diagnosis for conduct disorder (1 subj.), attention deficit hyperactivity disorder (ADHD) (2 subj.) or attention deficit disorder (ADD) (1 subj.), unsuccessful earlier examinations because of restlessness (1 subj.), native language other than Finnish (6 subj.). B) Exclusion criteria: metal in body (1 subj.).

We recruited age- and gender-matched controls for the EPB participants, therefore 6 TB children were not invited to participate in the experiment. NICU, neonatal intensive care unit.

**Figure 2** Experimental design and behavioral performance of visual attention and WM tasks in 7.5-year-old TB and EPB children. (A) Design of the visuospatial n-back tasks. The match targets for 0-, 1- and 2-back tasks are marked with arrows. (B) Response times, percent incorrect responses, and evaluation of the difficulty level of the tasks. The TB children responded slower but made less mistakes in the tasks than the EPB children. There were no significant differences between the groups in the evaluation of the difficulty level of the tasks. EPB, extremely prematurely born; TB, term-born; 0, 1 and 2 in the lower panel refer to 0-, 1- and 2-back tasks. \* $P = 0.043$ , \*\* $P = 0.006$ . Error bars indicate standard error of the mean.

**Figure 3** Whole-brain activation patterns in TB and EPB children. (A) Attention-related brain areas detected by contrasting the 0-back task with visual fixation baseline (Rest). (B) WM-related brain areas shown by the contrasts 1-back > Rest and 2-back > Rest, and WM load-related brain activation detected by directly contrasting 2-back and 1-back tasks. (C) Significant group differences in the 0-back attention task and (D) a significant group effect in

the 1- and 2-back WM tasks. (E) Mean signal change in the ROI consisting of voxels that were more activated in EPB than TB children (red circle). The columns illustrate the mean percent signal change in the ROI in the 1- and 2-back tasks. Activation in the selected slice planes is displayed on the MNI standard brain. The data were thresholded at  $Z > 2.58$ , GRF corrected cluster  $P < 0.05$ . EPB, extremely prematurely born; TB, term-born; 1 and 2 refer to 1- and 2-back tasks. R, right.

**Figure 4** Correlations between BOLD signal changes and WM performance. In EPB children, incorrect responses in the 2-back task correlated negatively with the signal change in the left PFCdl and PFCmed. The approximate locations of the ROIs are indicated with red spheres on the selected slice planes of the MNI standard brain. EPB, extremely prematurely born; TB, term-born; PFC, prefrontal cortex; dl, dorsolateral; med, medial; R, right. The correlation was statistically significant in the PFCmed ( $P = 0.024$ , after Bonferroni correction with 6), but in PFCdl, the  $P = 0.018$  did not survive Bonferroni correction with 6.

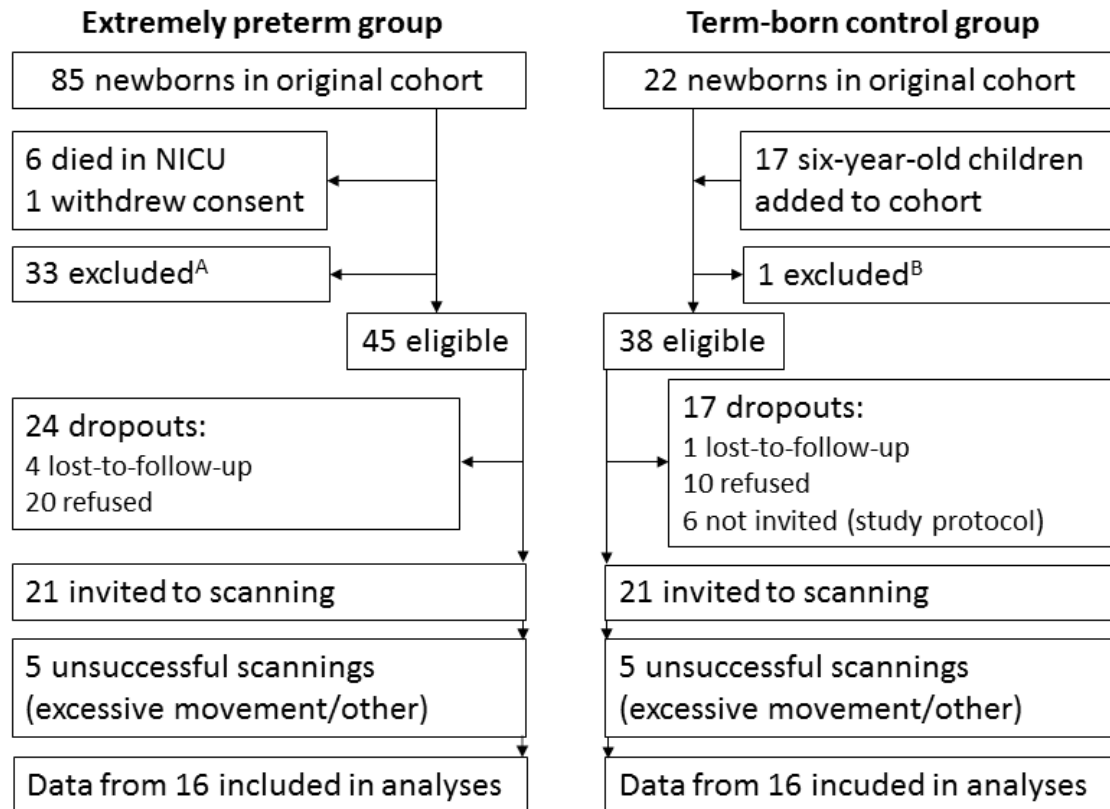
**Figure 5** Group differences in FA, MD, AD and RD values. TBSS analysis ( $P < 0.05$ , TFCE-corrected) showed (A) higher FA values in several white matter tracts in EPB compared with TB children including the superior longitudinal fasciculus (SLF), inferior fronto-occipital fasciculus/inferior longitudinal fasciculus (IFO/ILF), cortico-spinal tract (CST) and cerebellar white matter. (B-D) demonstrate lower MD, AD and RD values in EPB than TB children in several of these white matter tracts. The statistical maps are superimposed on the mean FA skeleton (green) overlaid on the mean FA image of all children. The horizontal lines in the sagittal brain slice indicate the level of selected axial slice planes that are presented in the frames with the corresponding colors. EPB, extremely prematurely born; TB, term-born; AD,

axial diffusivity; CERip, inferior cerebellar peduncle; FA, fractional anisotropy; MD, mean diffusivity; PCT, pontine crossing tract; RD, radial diffusivity; R, right.

**Figure 6** Correlations of the whole-brain voxelwise FA, MD and RD with response times of the WM tasks in TB children. (A) In the 1-back task, faster RTs were associated with higher FA values, and lower MD and RD values in several white matter tracts including the superior longitudinal fasciculus (SLF) and cortico-spinal tract (CST). (B) In the 2-back task, faster RTs were associated with higher FA values. The statistical maps are superimposed on the mean FA skeleton (green) overlaid on the mean FA image of all children. The scatter plots show the mean of each DTI-parameter extracted from all significant voxels in each child. The horizontal lines in the sagittal brain slice indicate the level of selected axial slice planes that are presented in the frames with the corresponding colors. TB, term-born; FA, fractional anisotropy; MD, mean diffusivity; RD, radial diffusivity; RTs, response times; R, right.

**Figure 7** Correlations of the whole-brain voxelwise FA, MD, AD and RD with neuropsychological test scores. (A) In TB children, lower numbers of errors in visual attention tests (inattention errors) were associated with lower MD, AD and RD values in several white matter tracts including the superior longitudinal fasciculus (SLF), inferior fronto-occipital fasciculus/inferior longitudinal fasciculus (IFO/ILF) and cortico-spinal tract (CST). (B) In EPB children, higher scores in a test of visuospatial processing (Block construction) were associated with lower FA values in the right cerebellar (CER) white matter. The statistical maps are superimposed on the mean FA skeleton (green) overlaid on the mean FA image of all children. The scatter plots show the mean of each DTI-parameter extracted from all significant voxels in each child. The horizontal lines in the sagittal brain slice indicate the level of selected axial slice planes that are presented in the frames with the

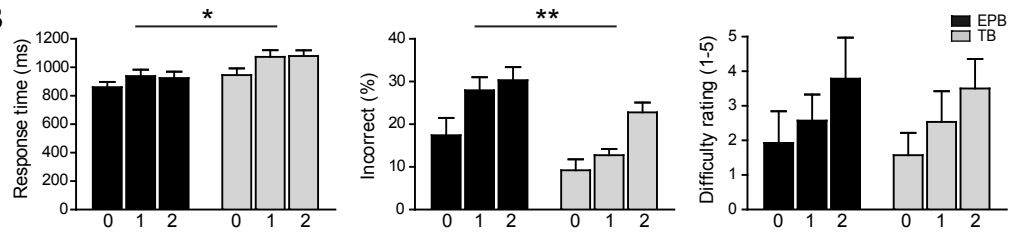
corresponding colors. EPB, extremely prematurely born; TB, term-born; AD, axial diffusivity; FA, fractional anisotropy; MD, mean diffusivity; RD, radial diffusivity; Vis., visual; R, right.

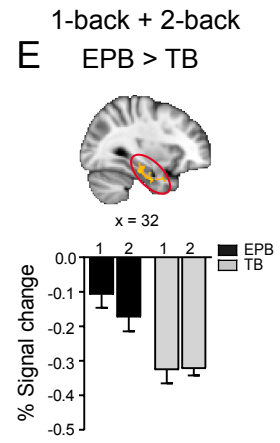
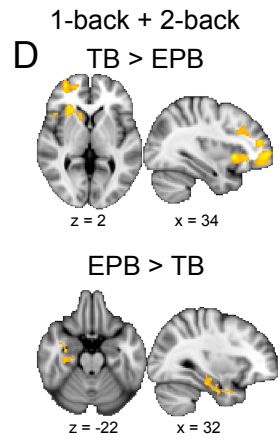
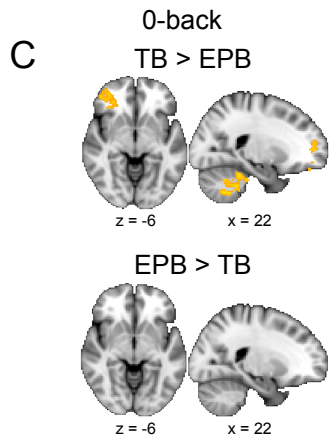
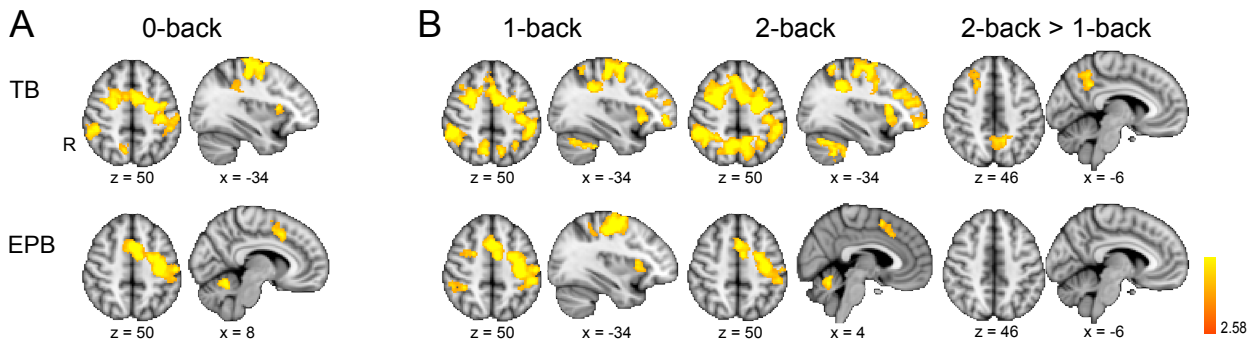


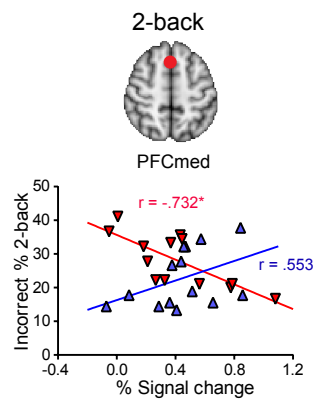
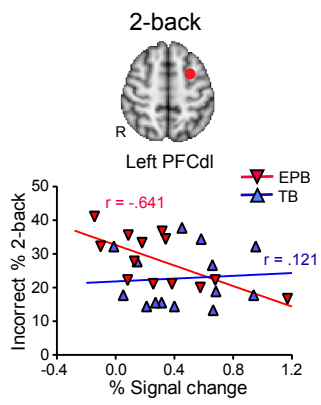
A



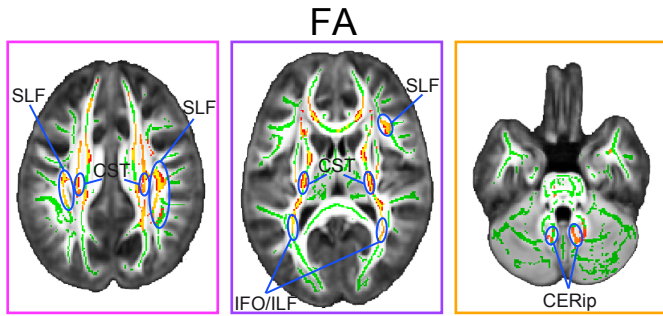
B



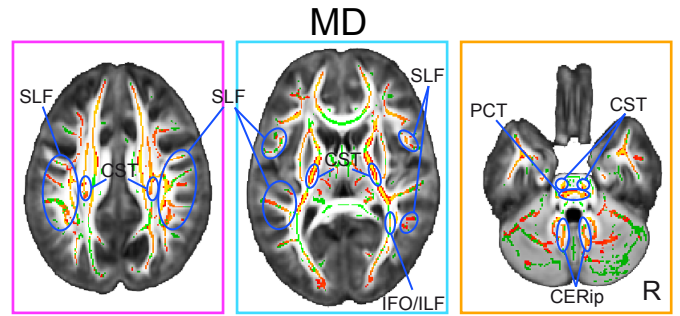




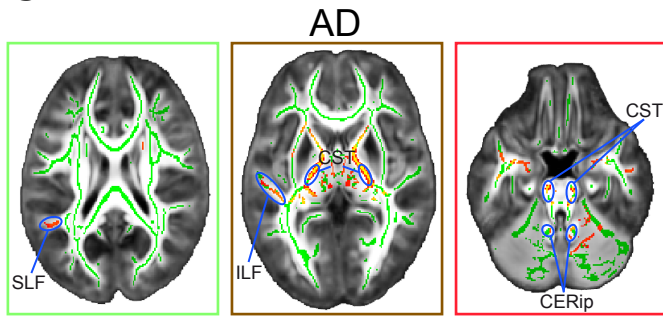
**A** EPB > TB



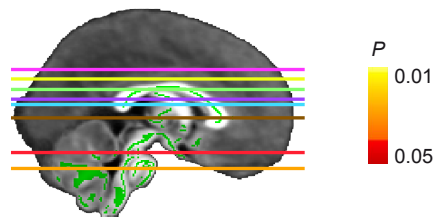
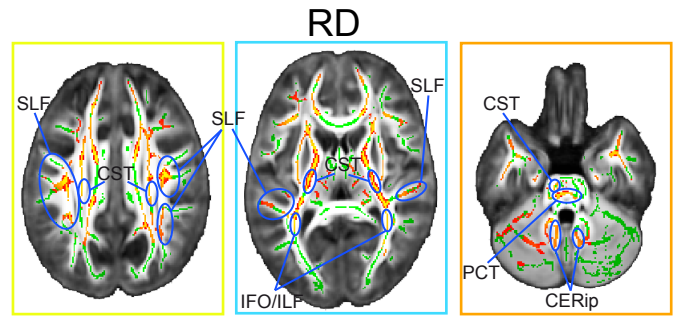
**B** TB > EPB



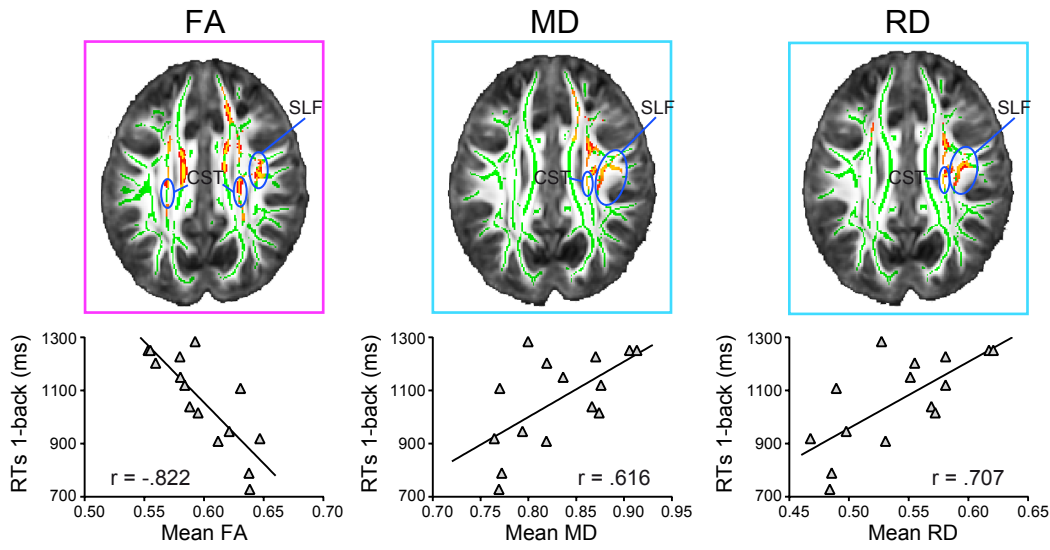
**C** TB > EPB



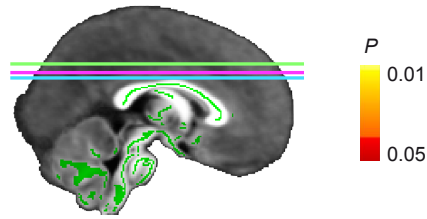
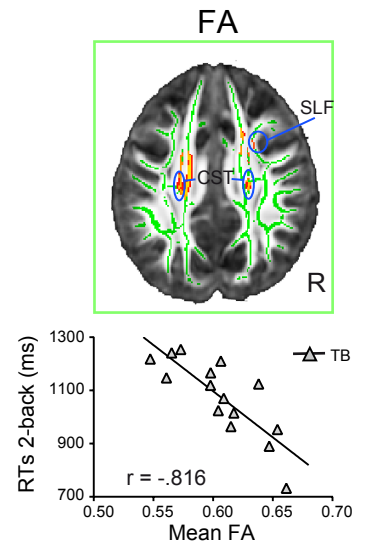
**D** TB > EPB

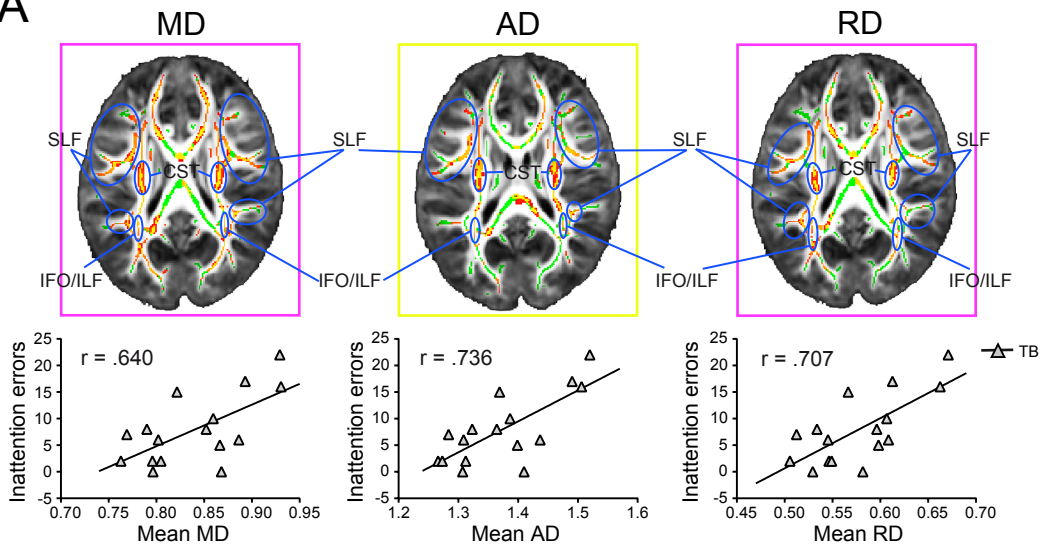
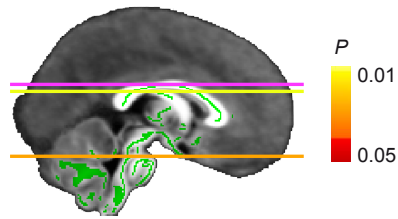
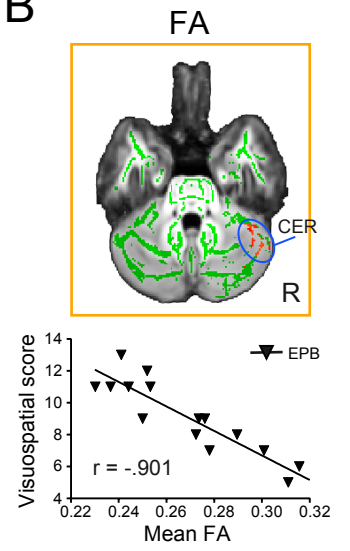


# A 1-back



# B 2-back



**A****B**

## Supplementary information

### Supplementary Table 1

The MRI evaluation of the EPB children (n = 16) at term equivalent age. All scans were classified by experienced neuroradiologists using a standardized scoring system consisting of eight 3-point scales (five for white matter and three for gray matter, Woodward et al., 2006).

Sub	Wmsa	Pv	Ca	Vd	tCC	Wmtot	Wmcl*	Gmsa	Cgmat	Sspa	Gmtot**
	1-3	1-3	1-3	1-3	1-3	sum	1-4	1-3	1-3	1-3	sum (n/a)
S1	1	1	1	1	1	5	1	1	1	1	3 (n)
S2	2	1	1	1	1	6	1	1	1	1	3 (n)
S3	2	1	1	1	1	6	1	1	1	1	3 (n)
S4	2	2	1	1	1	7	2	1	1	2	4 (n)
S5	2	2	2	1	1	8	2	1	1	1	3 (n)
S6	1	1	1	1	1	5	1	1	1	1	3 (n)
S7	1	1	1	1	1	5	1	1	1	1	3 (n)
S8	1	1	1	1	1	5	1	1	1	1	3 (n)
S9	1	1	1	1	1	5	1	1	1	1	3 (n)
S10	1	1	1	1	1	5	1	1	1	1	3 (n)
S11	1	2	1	2	2	8	2	1	1	1	3 (n)
S12	1	2	1	1	1	6	1	1	1	1	3 (n)
S13	1	1	1	1	1	5	1	1	1	1	3 (n)
S14	2	1	1	1	1	6	1	1	1	1	3 (n)
S15	2	1	1	1	1	6	1	1	1	1	3 (n)
S16	2	2	1	1	1	7	2	1	1	1	3 (n)

Ca, cystic abnormalities; Cgmat, cortical gyral maturation; Gmsa, gray matter cortical signal abnormality; Gmtot, total gray matter score; Pv, periventricular white matter volume loss; Sspa, size of the subarachnoid space; Sub, subject; tCC, thinning of the corpus callosum; Vd, ventricular dilatation; Wmcl, total white matter classification; Wmsa, white matter signal abnormality; Wmtot, total white matter score. \*Classification of white matter abnormality: 1 = none (score 5-6), 2 = mild (score 7-9), 3 = moderate (score 10-12), 4 = severe (score 13-15). \*\* Classification of gray matter abnormality: score 3-5 = normal (n), score 6-9 = abnormal (a).

## **Supplementary methods 1**

### **TORTOISE preprocessing**

For each subject, a high-resolution T2-weighted image underwent midsagittal alignment followed by AC-PC alignment using MIPAV 7.0.1 toolbox. The aligned T2 images were used as a reference for further registration of the diffusion weighted images (DWI). The diffusion gradients directions files were obtained for each subject using dcm2nii package of MRICron. For each phase-encoding direction, the corresponding raw DICOM images from scanner (45 volumes: 30 gradient directions at  $b=1000$  s/mm<sup>2</sup>, 6 directions at  $b=500$  s/mm<sup>2</sup>, 6 directions at  $b=300$  s/mm<sup>2</sup>, and 3 non-diffusion-weighted images at  $b=0$  s/mm<sup>2</sup>) were imported into TORTOISE DIFF\_PREP module and the voxel size was set to 1.5 mm isotropic voxels in the registration settings. The images underwent spatial preprocessing and the upsampled files of each phase-encoding dataset were fed into TORTOISE DR-BUDDI module to correct for susceptibility induced EPI distortions.

### **DTI-TK-Registration**

Tensorial datasets were fed into DTI-TK nonlinear registration pipeline. First, all the tensor images from both groups of children were selected for initial template computation, bootstrapped and resampled into 1.5 x 1.75 x 2.25 mm resolution (default setting in DTI-TK tutorial). The tensorial images were rigidly and affinely aligned to initial template using Euclidean Distance Squared similarity metric. Following this, tensorial images from all subjects were iteratively aligned to template with deformable registration, which was iteratively optimized for 6 times over the whole process. Supplementary Figure 2 illustrates the results of the DTI-TK registration pipeline.

## **Supplementary methods 2**

### **The ROI analysis of the right temporal lobe differential activation**

To investigate in more detail the group difference of stronger activation of the right temporal lobe regions in EPB than TB children (see Fig. 3D), we drew a ROI that included all voxels that were significantly activated in this contrast. This temporal lobe ROI had clusters of activation in the temporal pole (TP), PHG, Hipp and FG. The mean percent signal change values were extracted in each child in 1-back and 2-back task conditions and illustrated in the group level in the columns of Fig. 3E.

## Supplementary methods 3

### Validation of TBSS results

**1. Split sample analysis.** To test the within group consistency, we split the data samples of the TB children ( $n=16$ ) into two equal-sized subsamples and, by using TBSS, searched for any unexpected false positives by performing a direct comparison between the subsamples (8 TB vs. 8 TB) (Bach et al., 2014). As expected, there were no significant differences between the subsamples with the applied threshold ( $P < 0.05$ , TFCE corrected).

**2. Additional TBSS analysis using FSL.** Considering the impact of template selection and the registration of images on TBSS results (Keihaninejad et al., 2012), we performed an additional TBSS analysis. The FA images obtained by TORTOISE during tensor estimation were fed directly into FSL TBSS registration pipeline. These FA images were registered to a common template using FSL toolbox. During the registration step, a population-specific FA target template (most typical subject from the whole sample) was obtained and affine-aligned into 1 x 1 x 1 mm MNI152 standard space. Following this, each subject's FA image was nonlinearly transformed into the FA target and then affine-aligned into MNI152 space. The FA skeleton was obtained using the threshold of 0.2 and each subject's data were projected onto this skeleton. The group differences in FA values were estimated using an unpaired  $t$ -test with nonparametric permutation method with 5000 permutations. Statistical maps were thresholded at  $P < 0.05$  using a threshold-free cluster enhancement (TFCE) method with family-wise error (FWE) correction for multiple comparisons. The between group comparison showed significantly higher FA values in EPB than TB children (Supplementary Fig. 3).

**3. Analysis for potential outliers.** To test whether the results of group differences in TBSS analysis were caused by potential outlier datasets, we sequentially excluded each subject from the analysis and repeated the group comparisons. The results of this validation analysis showed that excluding a subject one-by-one did not globally affect (shift) the result presented in the main text; the directionality and the major locations of group differences remained the same as in the original analysis.

### References

Bach M, Laun FB, Leemans A, Tax CM, Biessels GJ, Stieltjes B, Maier-Hein KH. 2014. Methodological considerations on tract-based spatial statistics (TBSS). *Neuroimage*. 100:358-69.

Keihaninejad S, Ryan NS, Malone IB, Modat M, Cash D, Ridgway GR, Zhang H, Fox NC, Ourselin S. 2012. The importance of group-wise registration in tract based spatial statistics study of neurodegeneration: a simulation study in Alzheimer's disease. PLoS One. 7(11):e45996.

Woodward, L.J., Anderson, P.J., Austin, N.C., Howard, K., & Inder, T.E. (2006). Neonatal MRI to predict neurodevelopmental outcomes in preterm infants. New England Journal of Medicine, 355, 685-694.

## Supplementary results 1

### Alertness of the participants during scanning

After the imaging session, the children evaluated the level of alertness during the scanning. A two-way repeated-measures ANOVA showed that there were no significant differences in the reported alertness during scanning between the groups (main effect of group:  $F(1,26) = 1.47$ ,  $P = 0.236$ , partial  $\eta^2 = 0.05$ ) but there was a main effect of run on the reported alertness ( $F(2,52) = 6.04$ ,  $P = 0.004$ , partial  $\eta^2 = 0.19$ ). Both groups reported that they were alert during the first and second runs of the scanning, but felt some tiredness in the third compared to the first run ( $t(26) = 3.54$ ,  $P = 0.002$ , Cohen's  $d = 1.39$ ).

### Supplementary Table 2

Local maxima of the task-related fMRI activation areas of the whole-brain analysis when 0-back, 1-back and 2-back tasks were contrasted with fixation baseline and WM load-related fMRI activation areas (2-back > 1-back) in the EPB and TB children.

Region	Z	x	y	z
<b>TB children</b>				
<i>0-back &gt; Rest</i>				
<b>R Cer (V/VI)</b>	6.26	18	-50	-26
<b>L SFG: L/R MFG, SFG, SFGmed, L PreCG</b>	5.96	-20	-6	52
<b>R FP: MFG, OFC</b>	5.39	38	52	-8
<b>R SPL: PreCun</b>	4.80	12	-64	54

<b>R Ins:</b> PreCG, L/R IFGpo, Ins, Oper, Caud	4.76	34	16	6
<b>R SMG:</b> L/R AG, SMG	4.60	46	-36	48
<b>R MFG:</b> FP	4.55	42	44	22
<b>L Caud:</b> Oper, Ins, Thal	4.31	-18	8	16
<i>1-back &gt; Rest</i>				
<b>R SMG:</b> AG, SPL	6.69	46	-40	46
<b>L SFG:</b> L/R MFG, SFG, SFGmed, PreCG, L PostCG, SMG, SPL	6.56	-22	-4	54
<b>R Cer (V/VI)</b>	6.03	16	-48	-22
<b>L Ins:</b> Oper, PreCG	5.60	-30	24	-2
<b>R Ins:</b> IFGpo, OFC	5.60	30	18	4
<b>R FP:</b> MFG	5.57	38	54	-6
<b>L FP</b>	5.43	-36	50	-6
<b>R SPL/PreCun</b>	4.94	10	-66	52
<b>L MFG:</b> FP	4.56	-46	32	32
<b>L Cer (VI/Crus I)</b>	4.34	-32	-40	-38
<i>2-back &gt; Rest</i>				
<b>R MFG:</b> L/R CingG, SFG, SFGmed, MFG, PreCG SMG, SPL	6.65	34	4	54
<b>L Oper:</b> L/R Ins, OFC, IFGpo	5.82	-44	14	2
<b>R Cer (V/VI)</b>	5.60	16	-50	-22
<b>L MFG:</b> L/R FP	4.83	-34	28	24
<b>L Cer (VI/Crus I)</b>	4.48	-32	-56	-34
<i>2-back &gt; 1-back</i>				
<b>L PreCun/CingGPost:</b> SPL, L/R PreCun/CingGpost	4.88	-10	-50	36
<b>R SFG/MFG</b>	3.74	22	16	46
<b>L LOC</b>	3.68	-30	-74	26
<b>EPB children</b>				
<i>0-back &gt; Rest</i>				
<b>L PreCG:</b> SFG, MFG, PostCG, L/R CingG, SFGmed	5.70	-36	-20	50
<b>R Cer (V/VI)</b>	5.46	18	-52	-26
<i>1-back &gt; Rest</i>				

<b>L PreCG:</b> L/R SFG, MFG, CingG, SFGmed, PreCG	5.89	-36	-22	50
<b>R Cer</b> (V/VI)	4.99	20	-50	-26
<b>L Oper/Ins:</b> IFGpo, PreCG	4.92	-40	14	2
<b>R IFGpo:</b> Ins, Oper	4.53	58	12	16
<b>R SMG:</b> L/R SFG, SMG, SPL	4.21	52	-38	46
<i>2-back &gt; Rest</i>				
<b>L PreCG:</b> MFG, SFG, PostCG, SMG	5.61	-36	-20	50
<b>L/R CingG:</b> SFGmed	5.21	0	10	54
<b>R Cer</b> (V/VI)	4.45	18	-52	-24
<i>2-back &gt; 1-back</i>				
-	-	-	-	-

---

The MNI coordinates and Z-values are reported for the local maxima of the anatomical areas included in the significantly activated voxel clusters. The brain area corresponding to peak voxel is written in bold and the anatomical areas included in the voxel cluster are written in regular. EPB, extremely prematurely born; TB, term-born; AG, angular gyrus; Caud, caudatus; Cer, cerebellum; CingG, cingulate gyrus, FP, frontal pole; IFG, inferior frontal gyrus; Ins, insula; LOC, lateral occipital cortex; MFG, middle frontal gyrus; OFC, orbitofrontal cortex; Oper, opercular cortex; PreCG, precentral gyrus; PreCun, precuneus; PostCG, postcentral gyrus; SFG, superior frontal gyrus; SMG, supramarginal gyrus; SPL, superior parietal lobule; Thal, thalamus; med, medial part; po, pars opercularis; post, posterior part; L, left; R, right.

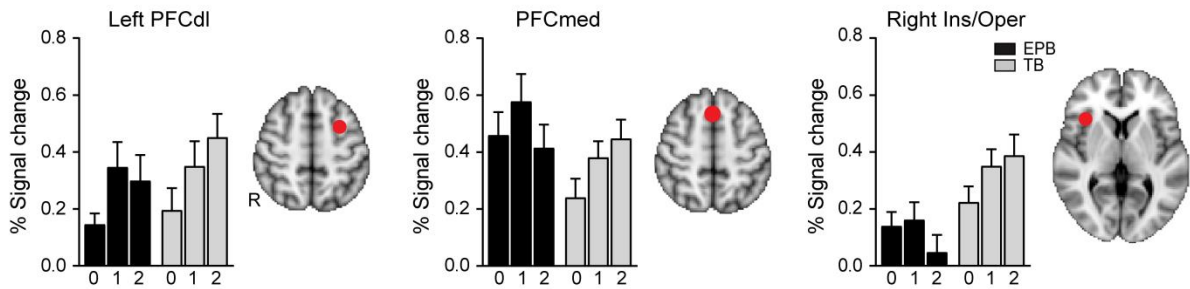
### Supplementary Table 3

Local maxima of the group differences in the 0-back task between EPB and TB children, and of brain regions that in the two-way ANOVA showed a significant main effect of memory load (2-back > 1-back) and significant group differences.

Region	Z	x	y	z
<b>Attention task (0-back &gt; Rest)</b>				
<i>TB &gt; EPB</i>				
<b>R FP: OFC</b>	3.86	20	54	6
<b>R Cer (V/VI): PHG</b>	3.73	20	-40	-24
<i>EPB &gt; TB</i>				
-	-	-	-	-
<b>ANOVA</b>				
<i>TB children &gt; EPB children</i>				
<b>R OFC: MFG, FP, IFGpo, Ins, Caud</b>	4.62	30	30	-2
<i>EPB children &gt; TB children</i>				
<b>R PHG: Hipp, TP, STG, FG</b>	3.63	36	-2	-28
<i>2-back &gt; 1-back</i>				
<b>L PreCun</b>	3.66	-10	-50	38

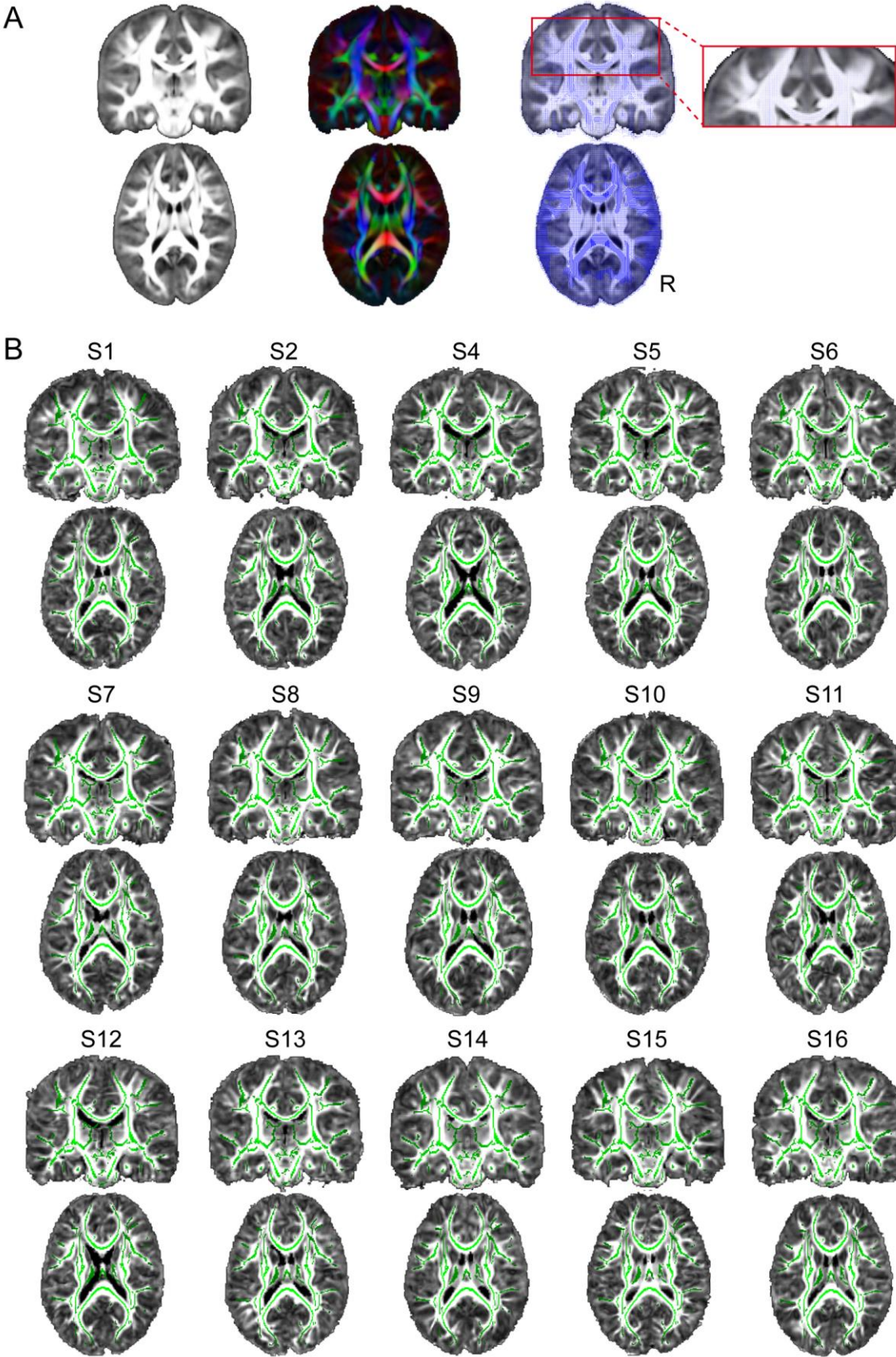
The MNI coordinates and Z-values are reported for the local maxima of the anatomical areas included in the significantly activated voxel clusters. The brain area corresponding to peak voxel is written in bold and the anatomical areas included in the voxel cluster are written in regular. EPB, extremely prematurely born; TB, term-born; Caud, caudatus; Cer, cerebellum; FG, fusiform gyrus; FP, frontal pole; Hipp, hippocampus; IFG, inferior frontal gyrus; Ins, insula; MFG, middle frontal gyrus; OFC, orbitofrontal cortex; PHG, parahippocampal gyrus; PreCun, precuneus; STG, superior temporal gyrus; TP, temporal pole; po, pars opercularis; L, left; R, right.

## Supplementary Figure 1



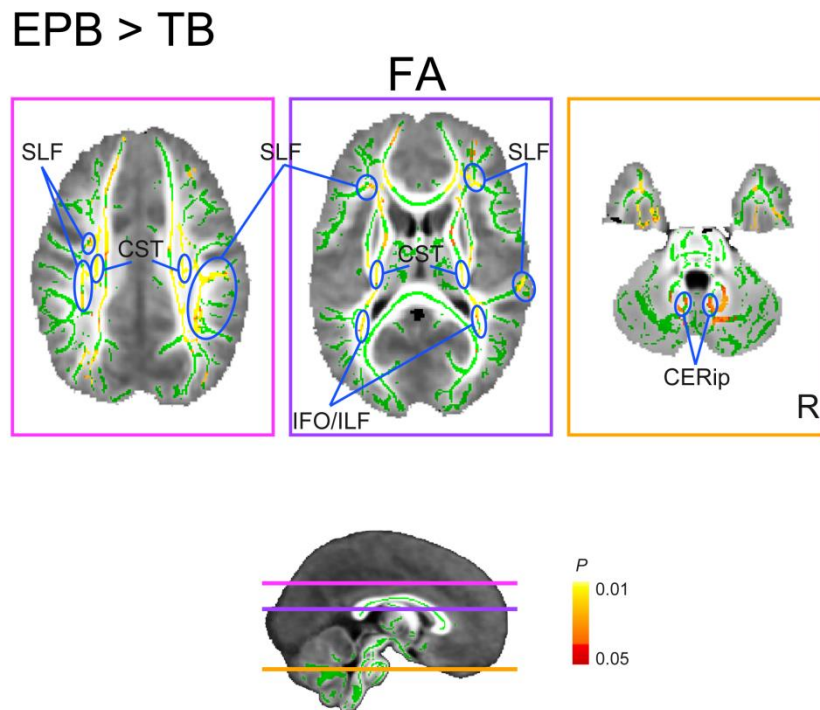
**Supplementary Figure 1.** Attention (0-back) - and WM (1-back and 2-back) -related mean signal changes in the left PFCdl, PFCmed and right Ins/Oper ROIs in TB and EPB children. The approximate locations of the ROIs are indicated with red spheres on the selected slice planes of the MNI standard brain. The columns illustrate the mean percent signal change in each ROI in each task. EPB, extremely prematurely born; TB, term-born; 0, 1 and 2 refer to 0-, 1- and 2-back tasks. Ins/Oper, insular/opercular cortex; PFC, prefrontal cortex; dl, dorsolateral; med, medial; R, right.

Supplementary Figure 2



**Supplementary Figure 2.** A) Coronal and axial slices of the mean FA template of all EPB and TB children (left), the RGB-color coded mean FA template (middle), and a template map of principal diffusion tensor directions, with an inset illustrating the corpus callosum (right). B) The mean FA skeleton overlaid on each (preterm-born) individual's normalized FA map. The individual FA maps demonstrate that the major fiber tracts such as the corpus callosum are aligned with the template's skeleton. S1 – S16 refer to the preterm subjects. The code is the same as is used for the subjects in Supplementary Table 1. DTI was not obtained from S3 explaining why no individual FA map is shown for this subject. R, right; S, subject.

**Supplementary Figure 3**



**Supplementary Figure 3.** Group differences in FA values using FSL's TBSS analysis. Higher FA values were found in several white matter tracts in the EPB compared with TB children ( $P < 0.05$ , TFCE-corrected). The statistical maps are superimposed on the mean FA skeleton (green) overlaid on the mean FA image of all children. The horizontal lines in the sagittal brain slice indicate the level of selected axial slice planes that are presented in the frames with the corresponding colors. EPB, extremely prematurely born; TB, term-born; CERip, inferior cerebellar peduncle; CST, cortico-spinal tract; FA, fractional anisotropy; IFO/ILF, inferior fronto-occipital fasciculus/inferior longitudinal fasciculus; SLF, superior longitudinal fasciculus; R, right.